PHYSICO-CHEMICAL STUDIES OF SYNTHETIC OXYGEN CARRIERS

DISSERTATION

Submitted in Partial Fulfilment of the Requirements
for the Award of the Degree of

Master of Philosophy

IN

CHEMISTRY

BY

SABA BEG

Under the Supervision of

Dr. Afaq Ahmad

DEPARTMENT OF CHEMISTRY
ALIGARH MUSLIM UNIVERSITY
ALIGARH (INDIA)

1990

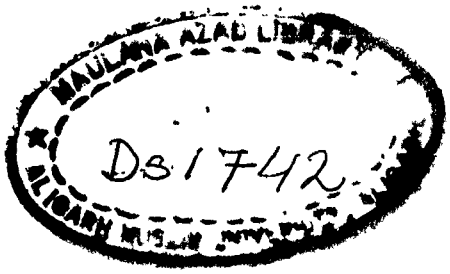

PHONE : 25515

DEPARTMENT OF CHEMISTRY
ALIGARH MUSLIM UNIVERSITY
ALIGARH—202 002

This is to certify that the dissertation entitled 'Physico Chemical Studies of Synthetic Oxygen Carriers' submitted to the Aligarh Muslim University, is the original work of Ms. Saba Beg, carried out under my supervision and is suitable for the award of M.Phil degree in chemistry.

Afaq Ahmad

(Dr. Afaq Ahmad)

ACKNOWLEDGEMENT

I wish to express my deep sense of gratitude to Dr. Afaq Ahmad, Department of Chemistry, Aligarh Muslim University, for his valuable guidance, untiring help and constant encouragement in carrying out this work.

I am also grateful to Prof. S.A.A. Zaidi, Chairman, department of chemistry for providing the necessary facilities.

Saba Beg
(Saba Beg)

C O N T E N T

CHAPTER - I

INTRODUCTION

The reversible oxygen carries are compounds which can take up and release molecular oxygen reversibly. Such compounds in the form of metal chelates occur in nature in small numbers. These are extremely important to life processes particularly respiration and are hence found in all living organimsm, both plants and animals. Hemoglobin and the less common hemocyanins are the well known natural oxygen carriers. The complicated chemical structure of these proteins render themselves difficult for investigation. As such, the study of synthetic oxygen carriers may be of considerable help in this connection, since they can be readily investigated by chemical and physical means. Such model compounds are known in small numbers and include (a) bissalicylaldehyde - ethylenediimene cobalt (II) and its derivatives and (b) the cobalt - histidine chelates.

The development of synthetic oxygen carrying compounds is quite recent and thus for restricted to chelates of cobalt. The affinity of a synthetic cobalt chelate for molecular oxygen was first discovered by Pfeiffer et al [1] when they observed that red brown crystals of bis-salicylaldehyde-ethylenediimine cobalt (II) darken on exposure to air. Tsumaki [2] concluded that the change in colour was due to reversible absorption of molecular oxygen. A large number of cobalt chelates [3,5] are

since found to be capable of reversible reaction with oxygen both in the solution [7] and in the solid state [4,6]. The first synthetic aqueous cobalto - histidine compound capable of acting as a carrier for molecular oxygen was reported by Burk et al [8]. It has been found that only cobalt histidine chelate combines reversibly with molecular oxygen and chelates of Cu^{++}, Ni^{++}, Fe^{++} and Mn^{++} with histidine do not show this property [9], while copper (II) and nickel (II) derivatives remain unaffected. The iron (II) derivative was oxidised irreversibly to the iron (III) state; and resulted in the precipitation of ferric hydroxide.

Dean Burk, J. Hearon, L. Caroline and A.L. Schade [8] observed that cobalt was found to be an effective inhibitor of growth and respiration of various aerobic and anaerobic microorganisms and animal tissues and tumors and its physiological action may be overcome reversibly and rather specifically by histidine among natural amino acid tested [10]. The formation of a red complex in alkaline solutions containing cobalt and glycylglycine (GG) was first observed by Smith [11] who believed that it might be an intermediate in the cobalt - catalysed enzymatic hydrolysis of glycylglycine. Hearon, Burk [12] studied extensively the uptake of oxygen by cobalt histidine chelate in solutions. Similar studies were carried out with GG, peptides of histidine and a number of other amino acids.

They observed that the yellow-brown complexes of GG and histidine are reversibly oxygenated and change spontaneously into the pink colour, irreversible oxidation forms.

Admission of O_2 to pink or blue solution of octahedral cobalt (II) complex rapidly yields yellow or at high concentration brown solutions of binuclear oxygenated complexes. Depending upon the ligands these complexes decompose at a variety of rates to yield red mononuclear cobalt chelates.

The coordinating ion must be capable of existing in more than one oxidation state [15]. However, if the oxidation potential of the ion is too high (the tendency to loose an electron is very great), then irreversible oxidation of the, ion to a higher valence state will occur. Accordingly it is necessary to have ions that have oxidation potential lying in a certain range so that there is some donation of electrons to oxygen molecule but not enough to cause irreversible oxidation. The oxidation potential of the ions can be so adjusted by chelation with the proper ligands. It would be possible therefore, to predict which chelates would act as oxygen carriers if the oxidation potentials of the chelates in given solvent system were known and steric factors were considered. Unfortunately at this time very few oxidation potential data have been reported for non aqeous system or for any but the more common ligands.

J.B. Gilbert, M. Clydeotey and V.E. Price [13] investigated formation and composition of red cobalt complexes of glycyldehydroalanine, glycyl-D- and glycyl-L-alanine and glycylglycine and studied their enzymatic hydrolyses. The composition of these complexes were examined and the red complex of glycylglycine was crystallized and characterized. Formation of the red colour actually indicates the ability of the peptide to form an oxygenated complex with Co^{++} and does not necessarily indicate the relative ability of Co^{++} to coordinate with peptide. The formation of this red complex does not occur under anaerobic condition and the absorption maximum was at 520 mμ. A portion of the glycylglycine originally added was not enzymatically hydrolyzable and the amount of free cobaltous ion in solution was reduced. By varying the concentration of Co^{++} and GG, the intensity of red colour was related to the amount of Co^{++} bound, oxygen consumed and glycylglycine rendered unhydrolyzable. The results indicated that 2 moles of GG and 0.5 mole of oxygen combine with 1 mole of cobalt to form the red complex. The oxidation was not reversible on acidification to pH 2.

Addition of cobaltous ion to solution of glycyldehydroalanine (GDA) produces first a yellow brown and then a red colour [14] complex. The same colour changes occur when Co^{++} is added to glycyl-L-alanine (L-GA) and glycyl-D-alanine (D-GA). The appearence of a red colour with a maximum absorption at 520 mμ

in solution of GG and Co^{++} has been described by Smith [6] and a possible correlation between the binding of this metal and the enzymatic susceptibility of the substrate was suggested. Hearon Burk, et al [12, 15] have studied extensively the uptake of oxygen in solutions of Co^{++} and histidine. Similar studies have been carried out with GG peptides of histidine, and a number of other amino acids. These authors have shown that the yellow-brown complexes of glycylglycine and histidine are reversibly oxygenated and change spontaneously into the pink, irreversible oxidation forms.

The rate of formation of the stable red complex between cobalt, GG and molecular oxygen has been investigated over the range of pH 7 to 12.5 [16]. It was observed that the formation of this complex proceeded through an intermediate, a complex containing two hydroxyl ions, $[(OH)(GG)_2Co\text{-}O_2\text{-}Co(GG)_2(OH)]^{=}$. Below pH 8 this intermediate was reported to be highly unstable and its presence could be deduced only from the pronounced pH dependence of the reaction rate. At higher pH ranges the intermediate became increasingly stable and was observed by its intense brown colour. The important step in the formation of the intermediate is the addition of oxygen to $Co(GG)_2(OH)_2^{=}$, with a rate constant about 6×10^4 $(\text{moles/litre})^{-1}$ min^{-1}, at ionic strength 1.0 at $25^{\circ}C$.

Gilbert, Otey and Price made the important discovery that

oxygen was taken up in the formation of the complex and that it could not be formed in the absence of molecular O_2. They obtained the analytical data to show that the complex contained Co, GG and molecular O_2, in the ratio 2:4:1. Thus this complex was similar to the cobalt-histidine-oxygen complex studied by Hearon, Burk and Coworkers and to the peroxo cobalt ammines described by Werner and Mylius. Possible structures for the complex in solution given by Price are the I II, latter formation.

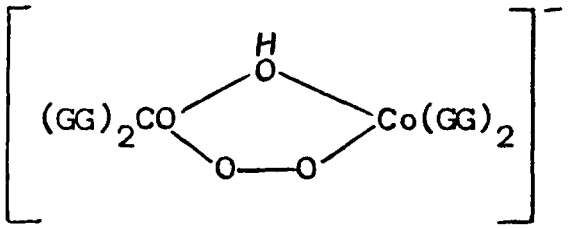

(I)

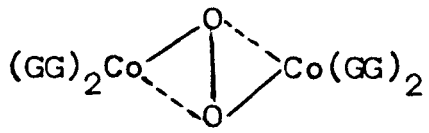

(II)

is similar to one suggested for the cobalt-histidine-oxygen complex.

The study of kinetics of this red complex over the range of pH 7.0 to 12.5 was conveniently divided into two parts: at low pH, where the red complex is formed directly and at high pH, where as already observed by Gilbert, Otey and Price, a brown coloured intermediate occurs. Throughout the entire pH range, i.e. whether or not the brown intermediate is observed, the final product, in solution is identical spectroscopically, with the products obtained by Smith and of Gilbert, Otey and Price.

In the pH region 7 to 8 the brown intermediate did not appear in detectable amounts. The conversion of the red product and the absorption of oxygen both occur slowly. Strict adherence to Beer's law was observed on measuring the absorbance, after the progressive dilution of the solution in which reaction had been completed at 520 mμ. This experiment shows that the absorption at 520 mμ, is an accurate measure of the concentration of the red product and that, in this pH range, it can be used to measure the rate of progress of its formation. In this range of pH, no pH changes were ever observed because of the excellent buffering action of the excess GG.

At high pH, above pH 8 as mentioned, a brown coloured species begins to be formed as a transient intermediate early in the reaction. As the pH is increased the brown colour appears more rapidly and becomes more intense, until, at sufficiently high pH, its appearance is instantaneous, the amount absorbed being 0.5 mole of cobalt, i.e. the same amount as is present in the final red product. It can therefore be concluded that at high pH all of the cobalt is instantaneously converted into the brown species and that this species already contains the Co-O-O-Co structure present in the final red product.

It was found by C. Tanford, Kirk and Chantooni [16] that the concentration, equilibrium constants and the rate constants

all depend on ionic strength. The reaction rate is influenced principally by the effect of ionic strength on the numerator.

In the low pH region the intermediate was assigned the formula II. The reaction mechanism deduced from the low pH data indicated that the formation of this intermediate would decrease with increasing pH. The intermediate thus becomes incresingly stable with increasing pH.

The brown coloured intermediate, containing the structure Co-O-O-Co, begins to make an appearence in the reaction mixture at pH 8. At sufficiently high pH all of the cobalt is instantaneously converted into this brown-coloured compound identical with the unstable intermediate of the low pH region i.e. that it too, is represented by structure II.

Some of the experiments in the unbuffered range of pH 10 to 11 were conducted with a view to measuring pH changes, rather than light absorption. The solutions were prepared in the complete absence of oxygen and their pH values measured. Oxygen was then buffered through the solution and the usual brown colour rapidly was formed. During this process a sharp drop in pH was observed. As the brown colour was transformed to the product, however an accompanying pH increase was found.

Qauntitatively, this result is in accord with the mechanism proposed earlier for the formation of II requires the absorption

of OH^- ions from the solution and these are released again in the transformation to I.

CHAPTER - II

METHOD OF CHEMICAL ANALYSIS

FAST REACTION KINETICS

The rate of a reaction, is defined as the rate of decrease of the concentration of a reactant or as the rate of increase of the concentration of the product. Thus, in kinetic investigations, the reactants are introduced in the reaction vessel and the concentration changes are followed with time. This so called static method of kinetic investigation is applicable only to reactions that are not too rapid and have half-lifes of at least several minutes.

Some reactions are fast and are over in a few seconds and cannot be followed manually. There are two main reasons why conventional techniques of static method fail to follow the rate of fast reactions:

(i) Reaction are started either by mixing the reactants or by raising the temperature of the reaction system. The time that it takes to mix the reactants or to bring them to a specified temperature may be significant in comparison to the half life of the reaction. An appreciable error therefore will be introduced since the initial time cannot be determined accurately.

(ii) The time that it takes to make a measurement of concentration during the kinetic run may be quite significant compared to the half life.

REACTIONS IN FLOW SYSTEM

In cases where one desires to study a reaction at extremely low concentration, a stream of reaction mixture is passed through a reaction vessel, known as reactor, to obtain enough product for analysis. The flow systems are of two general type. In the first, there is no stirring and is known as plug flow. In the second there is stirring which is sufficiently vigorous to effect complete mixing within the reactor.

TECHNIQUES FOR VERY FAST REACTIONS

Some reactions are so fast that special techniques have to be employed. Such techniques are stopped flow and relaxation method.

STOPPED FLOW METHOD

The uncertainty in the time at which the reaction starts in usual techniques is overcome by special techniques devised to bring the reactants rapidly into the reactor and mix them quickly. One method, using the flow technique is the stopped flow method [17] shown schematically in Fig. 1. This apparatus is designed for the study of a reaction between two substances in solution. Solution of one of the reactants is maintained initially in the syringe A and the solution of the other in a syringe B. Syringe plungers are driven rapidly by a special device, The two solutions from the two syringes come out in the form of very fast

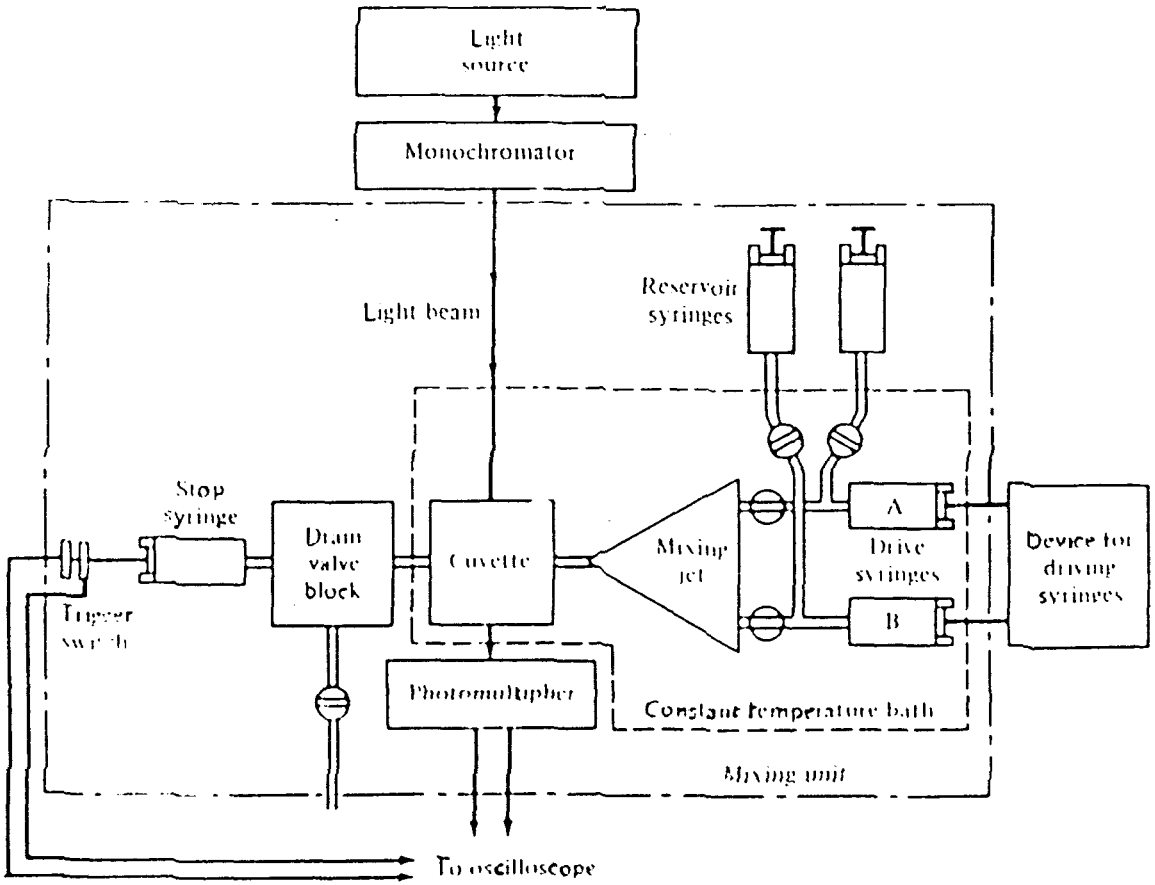

Figure 1. Schematic diagram of stopped-flow apparatus. Solutions in the two drive syringes A and B are forced rapidly through a mixing jet into a cuvette. When the flow is stopped, the oscilloscope is triggered and records light absorption as a function of time.

streams and impinge on each other in the mixing chamber. Mixing is complete in about 0.001 second. From the mixing chamber, the solution passes at once into the reaction cuvette. Sometimes mixing is done in the reaction cuvette itself. The concentration is monitored instantaneously using self recording spectrophotometric or some other physico-chemical technique like electrical conductivity, optical rotation or fluorescence. The data are directly recorded into the computer.

RELAXATION METHOD

The use of flow technique described above in the study of fast reactions is limited by the speed of mixing the solution. For hydrodynamic reasons it is impossible to mix two solutions in less than about 10^{-3}s. If half-life is less than this, the reaction is almost over before mixing has been achieved and under this situation the rate of measurement will be the rate of mixing and not the rate of reaction. The neutralization of strong acid and strong alkali in aqueous solutions, that is, the reaction

$$H^+ + OH^- \longrightarrow H_2O$$

under ordinary conditions has a half-life of 10^{-6}s, and its rate cannot be measured by stopped flow technique that involves mixing.

To overcome this difficulty the relaxation method is used [18]. The relaxation method differs from the conventional kinetic method in that the system is initially at equilibrium under a given set of conditions. These conditions are then suddenly disturbed, the system is no more at equilibrium and it relaxes to a new set of equilibrium. The speed with which it relaxes is measured.

Suppose that in the chemical reaction of interest we are able to monitor the concentration of a coloured species by passing light of the appropriate frequency through the mixture and observing the intensity of the transmitted beam. Consider a chemical reaction at equilibrium and suppose that the species we are monitoring has the concentration 'c' in Fig 2. Suppose that at time 't_o' one of the parameters on which the equilibrium depends (for example temperature) is instantaneously brought to some new value. Then the concentration of the species we are observing must achieve some new equilibrium value 'c'. Since chemical reactions occur at a finite rate, the concentration of the species will not change instantaneously to the new value, but will follow the course indicated by the dashed curve in Fig. 2. The system, having been perturbed from its old equilibrium position, relaxes to its new equilibrium condition.

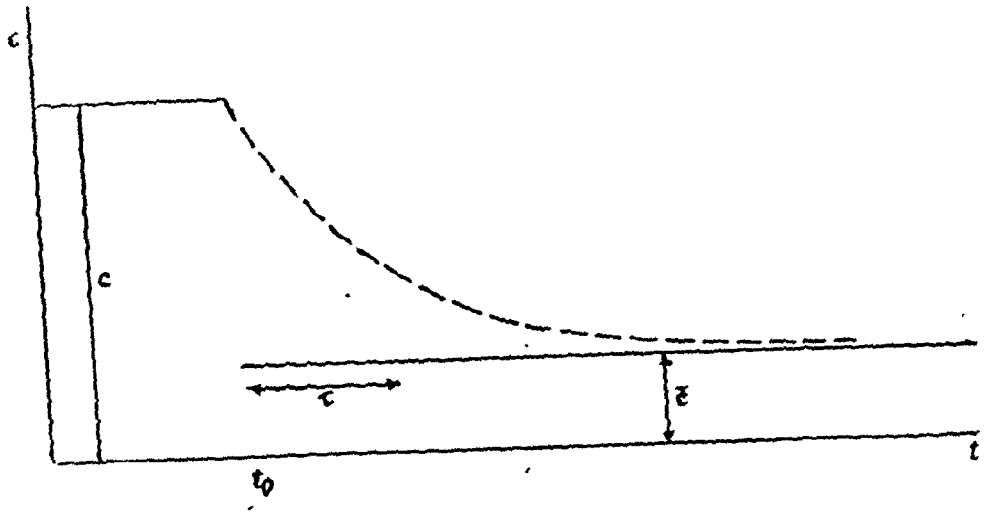

Fig. 2

Concentration change after impuls

As we will show, if the difference in concentration between th two states is not too large, then the curve in Fig. 2 is a sim exponential function, characterized by a single constant, the relaxation time, τ . The relaxation time is the time required for the difference in concentration between the two states to decay to 1/e of its initial value.

The apparatus for the 'temperature jump' method is shown schematically in Fig. 3. A high voltage power supply charges a capacitor, c. At a certain voltage the spark gap, G, breaks down and the capacitor discharges, sending a heavy current thr the cell and contains the reactive system at equilibrium in a conductive aqueous solution. The passage of the current raises the temperature of the system about $10^{o}C$ in a few microseconds.

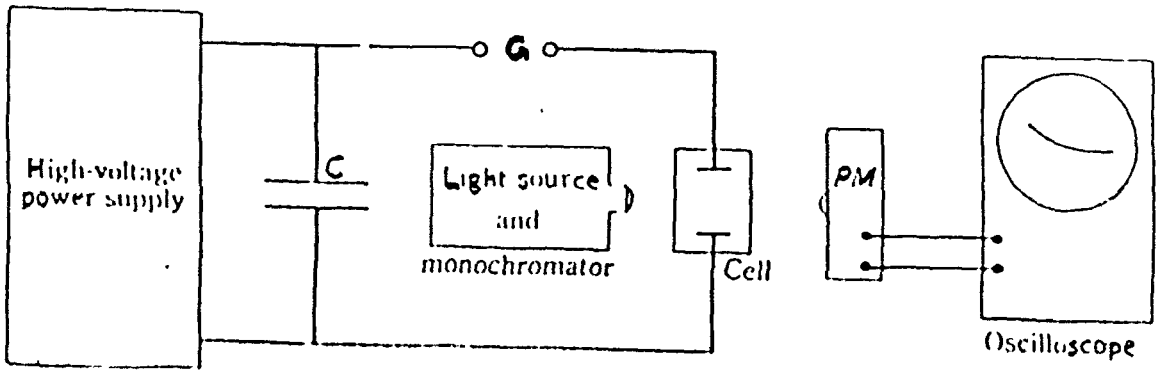
High-voltage
power supply
C
G
Light source
and
monochromator
Cell
PM
Oscilloscope

Fig 3

In the following time interval the concentration of the absorbing species adjusts to the equilibrium value appropriate to the higher temperature. This changes the intensity of the light beam emerging from the cell into the detecting photomultiplier tube, PM. The output of the photo-multiplier tube is displaced on the vertical axis of an oscilloscope; the horizontal sweep of the oscilloscope is triggered by the spark discharge. In this way the concentration versus time curve is displayed on the oscilloscope screen.

Consider the elementary reaction

$$A + B \rightleftharpoons C$$

The rate equation for this reaction can be written,

$$\frac{d\,(\xi/V)}{dt} = k_f C_A C_B + (-k_r C_c), \qquad \ldots (1)$$

in which we have expressed the net rate as the sum of the forward rate ($k_f C_A C_B$) and the reverse rate ($-k_r C_c$). It is convenient for graphical representation to give the reverse rate a negative sign here. The mole numbers and the concentrations of each species are expressed in terms of the advancement of the reaction,

$$n_A = n_A^o - \xi, \quad n_B = n_B^o - \xi, \quad n_C = n_C^o + \xi.$$

$$C_A = C_A^o - \frac{\xi}{V}, \quad C_B = C_B^o - \frac{\xi}{V}, \quad C_C = C_C^o + \frac{\xi}{V}.$$

The mole number, n^o, and the concentrations, C^o, are the values of these quantities at $\xi = 0$. When we use these values for the concentrations, equation (1) becomes

$$\frac{1}{V}\frac{d\xi}{dt} = k_f(C_A{}^o - \frac{\xi}{V})(C_B{}^o + \frac{\xi}{V}) + [-k_r(C_c{}^o + \frac{\xi}{V}].$$

from this equation it is evident that the forward rate is a quadratic function of ξ, while the reverse rate is linear function of ξ, these rates are shown as functions of in Fig. 4. The sum of the two functions is the net rate, indicated by the dashed line in Fig. 4.

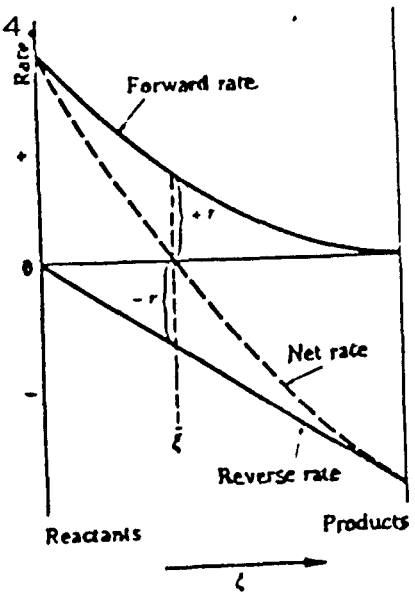

Forward, reverse, and net rate of reaction

Fig. 4

At $\bar{\xi}$, the equilibrium value of the advancement, the net rate is zero, and we have

$$r = k_f\bar{C}_A\bar{C}_B = k_r\bar{C}_c \qquad \ldots (2)$$

in which the bar over the concentration indicates the equilibrium value. The exchange rate, r, is the rate of either the forward or the reverse reaction (without the minus sign) at equilibrium. Equation (2) can be rearranged to the form

$$K = \frac{k_f}{k_r} = \frac{\bar{C}_c}{\bar{C}_A \bar{C}_B} , \qquad \ldots)(3)$$

which is the equilirium relation for the elementary reaction; K is the equilibrium constant.

Although the detailed shapes of the curves will depend on the order of the reaction, the forward rate, the reverse rate and the net rate of any elementary reaction will be related in the general way indicated in Fig. 4. Most importantly, it is apparent that the net rate can be approximated by a straight line over a narrow range near the equilibrium position. Let the net rate, $(1/V)\ (d\xi/dt) = v$. Then we expand v in a Taylor series about the equilibrium value of :

$$v = v_{\bar{\xi}} + \left(\frac{dv}{d\xi}\right)(\xi - \bar{\xi}).$$

However, $v_{\bar{\xi}}$ is the net rate at equilirbium, which is zero. Introducing the definition of v and multiplying by the volume, the equation becomes

$$\frac{d}{dt} = V\left(\frac{dv}{d\xi}\right)_{\bar{\xi}} (\xi - \bar{\xi}). \qquad \ldots (4)$$

we note that $V(dv/d\xi)_{\xi}$ has the dimensions of a reciprocal time, and depends only upon $\bar{\xi}$, that is, only upon equilibrium values of concentration, not upon ξ or t. We define the relaxation time τ, by

$$\frac{1}{\tau} = -V\left(\frac{dv}{d\xi}\right)_{\xi}. \qquad \ldots (5)$$

The minus sign is introduced to compensate the negative sign of the derivative.

The introduction of τ brings the rate equation (4) to the form

$$\frac{d\xi}{dt} = -\frac{1}{\tau}(\xi - \bar{\xi}), \qquad \ldots (6)$$

in which τ is independent of ξ or t. This equation has the form of a first-order law and integrates immediately to

$$\xi - \bar{\xi} = (\xi - \bar{\xi})_{o}\, e^{-t/\tau} \qquad \ldots (7)$$

in which $(\xi - \bar{\xi})_{o}$ is the initial displacement (at $t = o$) from equilirbium. Since the displacement of the concentration of any species from its equilibrium value is $\Delta C_i = C_i - \bar{C}_i$, and since $C_i = C_i^{o} + (v_i/V)_{\xi}$, where v_i is the stoichiometric coefficient of the species in the reaction, we obtain directly $\Delta C_i = (v_i/V)(\xi - \bar{\xi})$. Thus the displacement of the concentration of any species from the equilibrium value is proportional to the displacement of the advancement. Consequently, the time

dependence of the concentration of any species is given by the same relation as in equation (7)

$$(C_i - \bar{C}_i) = (C_i - \bar{C}_i)_o e^{-t/\tau} \qquad \ldots (8)$$

The pattern that appears on the oscilloscope screen in the temperature jump experiment is therefore a simple exponential one, provided only one reaction is involved. The value of τ can be obtained by measuring the horizontal distance (time axis) required for the value of the vertical displacement of fall to $1/e = 0.3679$ of its initial value Fig. 5.

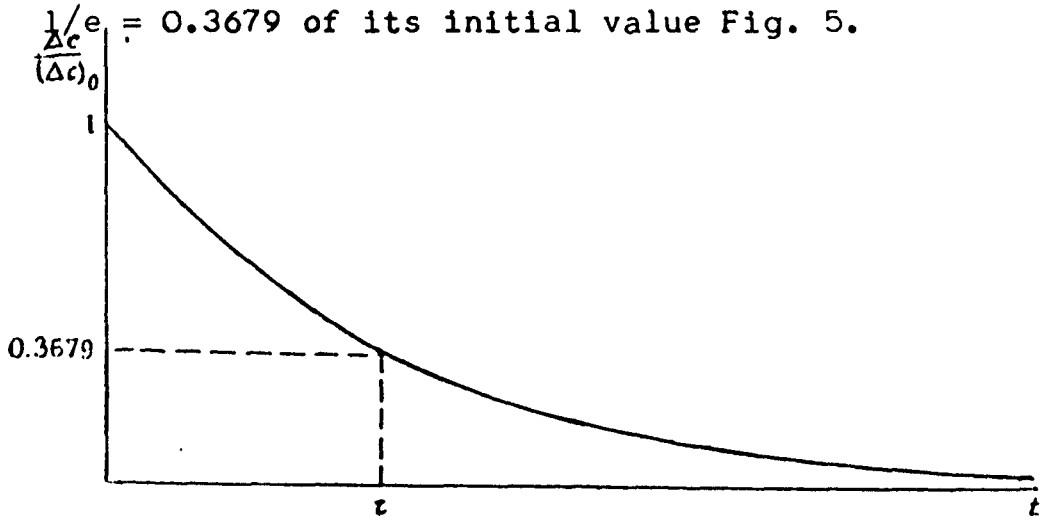

Fig. 5

The relaxation time

Equations (4) to (8) are quite general, they do not depend on the order of the reaction and most particularly they do not

depend on the example we chose for illustration. Equation (8) is a typical example of a relaxation law. It implies that any small perturbation from equilibrium in a chemical system disappears exponentially with time. If there are several elementary steps in the mechanism of a reaction then there will be several relaxation times. In this event, the expression for $C_i - \bar{C}_i$ is a sum of exponential terms such as that in equation (8). There is one such term for each relaxation time. The coefficient of each term and the relaxation times are determined by a computer fit of the data.

We can evaluate the relaxation time for the example above by evaluating the derivative, $dv/d\xi$, at $\xi = \bar{\xi}$. Since, $v = k_f C_A C_B - k_r C_c$, then

$$\frac{dv}{d\xi} = k_f C_A \frac{dC_B}{d\xi} + k_f C_B \frac{dC_A}{d\xi} - k_r \frac{dC_c}{d\xi} .$$

But $dC_A/d\xi = -1/V = dC_B/d\xi$, and $dC_c/d\xi = 1/V$. Thus, at $\xi = \bar{\xi}$, this becomes

$$\left(\frac{dv}{d\xi}\right)_{\bar{\xi}} = - \frac{k_f(\bar{C}_A + \bar{C}_B) + k_r}{V}$$

Then by the definition of τ, eq (5) becomes

$$\frac{1}{\tau} = k_f (\bar{C}_A + \bar{C}_B) + k_r \qquad \ldots (9)$$

By making measurements on the system with different values

of the equilibrium concentrations, we can evaluate both k_f and k_r. Knowledge of the equilibrium constant, in view of equation (3), provides additional information about k_f and k_r.

The relaxation method is not restricted to the study of very fast reactions. With apropriate choices of sensing and recording devices, we could use it to study the rate of any reaction. Relaxation technique is the only technique available for measuring rates of very fast reactions.

POLAROGRAPHY

The potential-current (voltametric) characteristics of polarized electrodes in solution gives the useful physical data as well as a means of analysis. The most widely studied and used method based on this principle is polarography [19]. Which permits quantitative and qualitative analysis of dilute solutions. Polarographic studies also can provide thermodynamic data for metal ion complexes and oxidation - reduction systems. A standard polarographic system consists of a large non-polarizable reference electrode and polarizable microelectrode such as dropping mercury electrode. A polarized electrode is an electrode which is forced to a potential other than the equilibrium potential of the bulk solution. The microelectrode is introduced in to the sample solution.

The dropping - mercury electrode has particular advantages for polarography, specifically (1) mercury has a high overvoltage for the reduction of hydrogen ions and thus extends the useful range of potential, (2) a dropping electrode presents a renewed and reproducible surface, and (3) the repetitive growth and falling of drops provide an average diffusion layer which is constant, as opposed to a fixed solid electrode which with time has an ever increasing diffusion layer.

The two electrodes polarography

Classically, dc polarography have been represented by a circuit of the kind shown in Fig. 6.

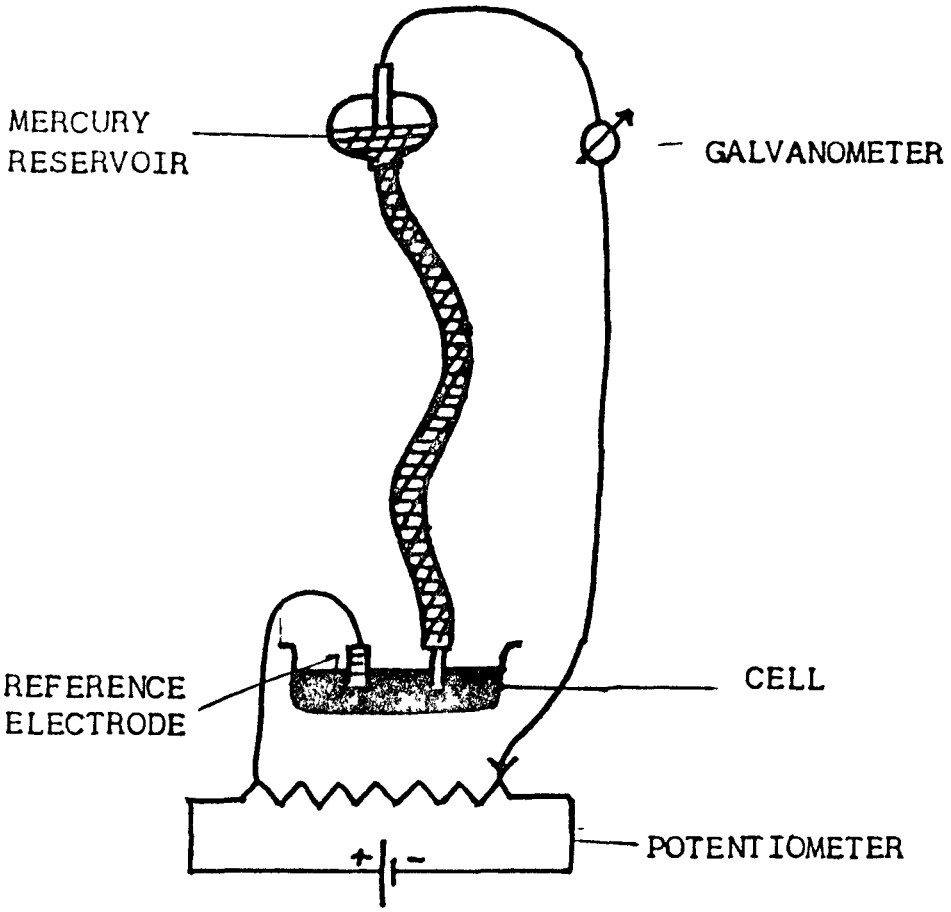

Fig. 6

In polarography, a dropping mercury electrode is dipped into an electrolysis cell, containing about 5 to 50 ml of solution. The inner diameter of the capillary is about 0.05 to 0.08 mm and the capillary is connected by tubing to a mercury reservoir, which is placed 30 to 80 cm, above the capillary orifice. By varying the height of the mercury head, the pressure

of the mercury column can be adjusted to give a drop time of about 2 to 8 sec. Atmospheric oxygen is removed from the solution by bubbling an inert gas such as nitrogen, hydrogen, or argon through the solution. A reference electrode is present in the solution alongwith the dme, and the electrochemical circuit is formed by connecting the cell of a potentiometer, which permits the application of any voltage across the dme and reference electrode. The resulting current flowing at potential E, is measured directly by means of a galvanometer or indirectly by measuring the potential drop across a standard resistor inserted in the circuit $\triangle$ graphical plot of mean current vs potential then gives the dc polarogram.

One of the greatest drawbacks in the classical two-electrode polarograph is that the potential is applied across the entire cell, rather than across the working electrode (dme in polarography) solution interface . Figure (7) shows the cell with a two-electrode potentiostat system incorporating IR compensation.

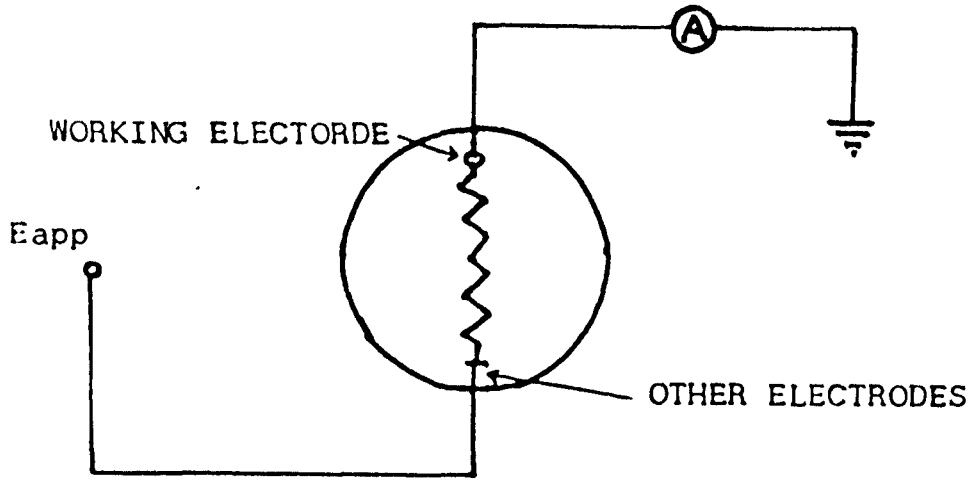

Fig. 7

The three electrode polarograph potentiostatic control

In two-electrode experiment, if the reference electrode is constructed properly, its potential relative to the solution will not change with current flow. The total potential applied to a cell will consist of the constant potential of the reference electrode, a potential between the solution and the working electrode (dme in polarography), and a potential through the solution owing to its resistance. Under these conditions the total current flowing through the cell will depend on the oxidation or reduction processes taking place at the working as a particular potential, as well as in the capacitive charging current required to change the double layer. Since the current flowing through the cell depends on the potential between the solution and the working electrode, it is important that this potential be well known and controlled. However, in the two-electrode arrangement, the potential which is actually controlled is that across both the working electrode and the reference electrode. The potential of the reference electrode is constant. Hence, the potential of the working electrode varies in the way as the total cell voltage, provided that the ohmic resistance of the solution does not cause an appreciable potential drop. This requires that the solution have either a low specific resistance of that the two electrodes be placed very close together. The three electrode system provided greater flexibility in the location of the reference and working electrodes and minimize the

effect of solution IR drop. In addition, it has the advantage that virtually no current passes through the reference electrode.

The general requirements for a three-electrode control system in polarographs are that it consists of the dme, a reference electrode and an auxiliary electrode, with the external circuit arranged so that potential control is maintained between the dme and the reference electrode, but so that cell current passes between the dme and the auxiliary electrode as shown in Fig. 8.

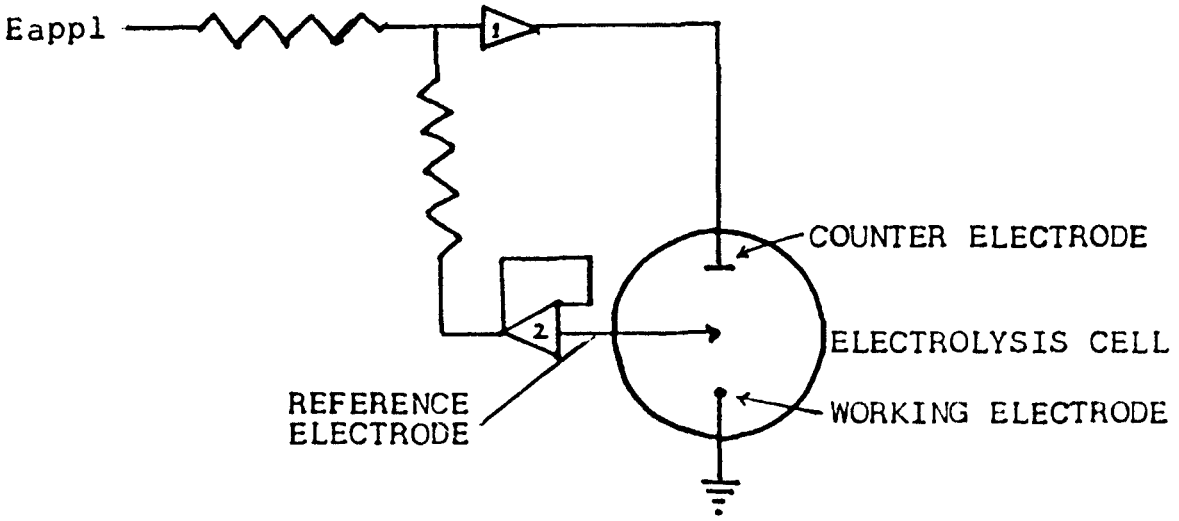

Fig. 8

The performance of an operational amplifier can be quantitatively understood by making two assumptions : (1) that the potential at the negative or inverting input is maintained equal to the voltage at the other input when the amplifier is

connected in a feed back configuration such as this (2) that no current flow in the amplifier from the negative input i.e. the amplifier behaves as if it had infinite input impedence. Of the polarographic analysis, differential pulse polarography is the most sensitive and powerful.

As shown in Fig. (9), in this technique a ramp is applied to the cell with a fixed - height modulation, pulse superimposed on it just before each drop is dislodged.

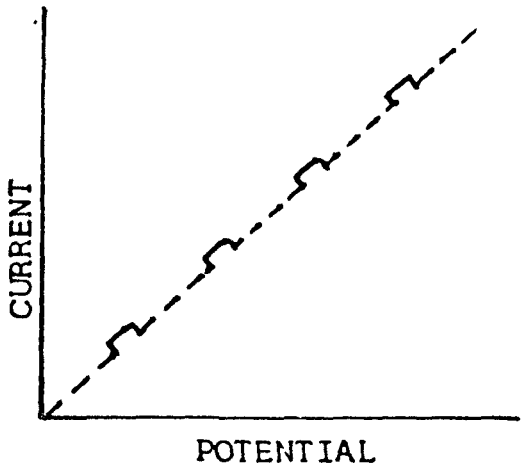

Fig. 9

Differential pulse excitation wave form

The current is measured twice for each drop, the first sample is taken just before the pulse ends. The two readings are then compared and the difference becomes the signal to be processed.

To a close approximation, the difference current varies

as the derivative of the polarographic wave, giving a peak out put presentation. Fig. (10) shows a typical differential pulse polarogram.

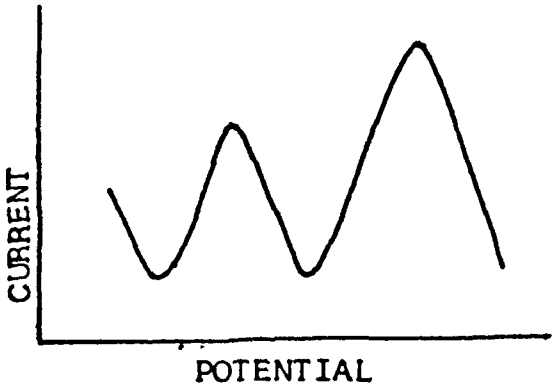

Fig. 10

Differential pulse polarogram

The amptitude of the modulation pulse effects the sensitivity and resolution. Higher the modulation pulse amplitude, the greater the peak height and the broader the peak width for a given concentration. Lowering the modulation pulse height narrows the width of the resulting peak and reduces its height.

Linear Diffusion and Linear Diffusion Currents

Diffusion is defined as the directed movement of a substance, under the influence of forces that arise from differences in concentration of the substance in various parts of the medium

[20]. The direction of diffusion is from regions of larger to smaller concentration and its rate is proportional to the magnitude of the concentration differences.

The simplest diffusion process is linear diffusion. Consider a linear diffusion cylinder as in Fig. (11), in which diffusion is proceeding upward in the negative x direction. The number of moles of the diffusing substance that diffuse across a given cross-sectional plane of area 'A' cm^2 in the infinitesimal interval of time dt is proportional to the concentration greadient dc/dx at the plane in question and is expressible by

$$dN = DA \frac{dc}{dx} dt$$

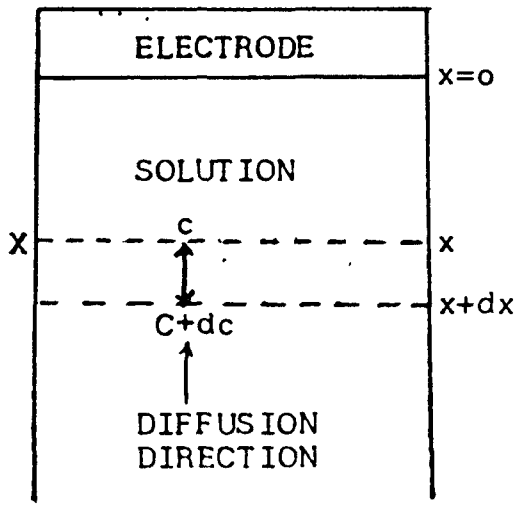

Fig. 11

Restricted linear diffusion to a flat electrode

The proportionality constant 'D' is the diffusion coefficient and it is evidently numerically equal to the number of moles of substance that diffuse across unit area in unit time when the concentration gradient is unity. This relation is referred to as Fick's First Law.

The change in concentration with time at a given plane at a given instant is given by

$$\frac{dc}{dt} = D \frac{\partial^2 c}{\partial x^2}$$

This is the fundamental differential equation for linear diffusion and it is sometimes referred to as Fick's second law. The instantaneous current at any time 't' after the e.m.f. is applied is given by

$$i_t = nFy\ CA \sqrt{\frac{D}{\pi t}}$$

where n is the number of faradays of electricity required per mole of electrode reaction and Fy is the Faraday (96,500 coulombs).

Symmetrical Spherical Diffusion

In symmetrical spherical diffusion the diffusing substance diffuses towards the center of a sphere along its radii. Consider a solid spherical electrode immersed in a solution of an electroreducible or electrooxidizable substance which is diffu-

sing to, and undergoing reaction at, the electrode. The diffusion field in this case is a spherical shell surrounding the electrode as shown in Fig. 12.

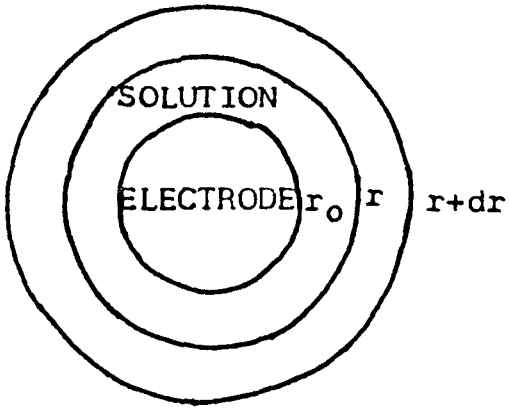

Fig. 12

Symmetrical spherical diffusion to a solid spherical electrode

Distance measured radially from the center of the spherical electrode is designated by r, and the radius of the electrode is designated by r_o.

Consider an infinitesimally thin shell of thickness dr at a distance r from the center of the electrode in Fig. 12. The area of the spherical surface at r is equal to $4\pi r^2$, and the number of moles dNr that diffuse across this surface in the time dt is given by the following expression, analogous to Fick's First Law,

$$dNr = 4\pi r^2 \quad D\left(\frac{\partial c}{\partial r}\right)_2 dt$$

and the flux at r is

$$f_r = \frac{dNr}{4\pi r^2 dt} = D\left(\frac{\partial c}{\partial r}\right)_r$$

The change in concentration in the spherical shell in the time dt is

$$dc = \frac{dN_{r+dr} - dN_r}{4\pi r^2 dr}$$

Therefore, the rate of change of the concentration with time at a given value of r and a given time t is

$$\frac{\partial c}{\partial t} = \frac{dN_{r+dr} - dN_r}{4\pi r^2 drdt}$$

The current at any instant is governed by the flux at the electrode surface, i.e., by the gradient at $r = r_o$. The concentration at the electrode surface at any time t is given by

$$\left(\frac{\partial c}{\partial r}\right)_{r=r_o,t} = C\left(\frac{1}{r_o} + \frac{1}{\pi Dt}\right) \approx \frac{f_{r=r_o}}{D}$$

The instantaneous value of the resulting current is, therefore,

$$i_t = nFy.4\pi r_o^2.f_{r=r_o}$$

$$= nFyADC\left(\frac{1}{r_o} + \frac{1}{\sqrt{\pi Dt}}\right)$$

Diffusion At The Dropping Mercury Electrode

Diffusion at a dropping mercury electrode is spherically symmetrical, but due to the periodic growth and fall of the mercury drops the area of the diffusion field changes continu-

ously during the life of a drop. The diffusion takes place in a medium that is moving with respect to the center of the drop, in a direction opposite to the direction of diffusion.

The fundamental differential equation which describes linear diffusion to a stationary flat electrode is

$$\frac{\partial c}{\partial t} = D \frac{\partial^2 c}{\partial x^2}$$

where the distance x is measured from the surface of the stationary flat electrode. Due to the incompressibility of the solution and the fact that the area of the diffusion field remain constant, the physical nature of linear diffusion to a moving flat electrode is exactly the same as that to a stationary flat electrode and the mathematical description of the diffusion is identical in the two cases.

On the other hand, this is no longer true in the case of symmetrical spherical diffusion to an expanding spherical, electrode (the dropping electrode), because, due to the expansion of the growing mercury drops, the area of the diffusion field at a given distance from the surface of the dropping electrode increases continuously with time during the life of each drop. Therefore, the equations that describe diffusion to the dropping electrode differ from those for stationary spherical diffusion by terms which describe the increase in the area of the diffusion field with time.

Ilkovic was the first to solve the complex probelm of diffusion to the dropping electrode, and to derive an equation for the resulting current. The Ilkovic equation was rederived by MacGillavry and Rideal, who obtained the same final expression for the diffusion current.

The fundamental differential equation for symmetrical spherical diffusion is

$$\frac{\partial c}{\partial t} = D \left[\frac{\partial^2 c}{\partial r^2} + \frac{z}{r} \left(\frac{\partial c}{\partial r} \right) \right]$$

in which r is radial distance measured on a fixed coordinate system whose origin is at the center of the spherical electrode. In order to apply this equation to diffusion at the dropping electrode the fixed coordinate r must be replaced by a moving coordinate, ρ, to take into account the increase in area of the diffusion field during the growth of the mercury drops.

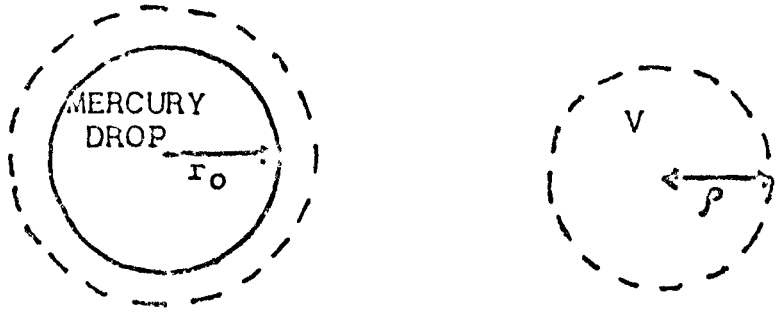

$$V = \frac{4}{3} \pi r^3 - \frac{4}{3} \pi r_o^3 = \frac{4}{3} \pi \rho^3$$

Fig. 13

Diffusion to a dropping electrode and definition of ρ (drawn to correct side)

MacGillavry and Rideal defined the moving coordinate ρ as the radius of a hypothetical sphere whose volume is the same as the volume enclosed between the surface of the growing mercury drop and a spherical surface of radius slightly larger than the radius of the drop, that is

$$\frac{4}{3}\pi r^3 - \frac{4}{3}\pi r_o^3 = \frac{4}{3}\pi\rho^3$$

$$\text{or } \rho^3 = r^3 - r_o^3$$

where r is the radial distance from a point in the solution to the center of the drop and r_o is the radius of the drop at any instant. This definition is represented pictorially in Fig. 13.

The flux at the surface of the drop is given by

$$(fr)_{\rho=o} = \frac{DC}{(rt)^{1/2}}\left(\frac{7r}{3\pi D}\right)^{1/2} = \frac{D^{1/2}C}{t^{1/2}}\left(\frac{7}{3\pi}\right)^{1/2}$$

and the expression for the current is

$$i_t = 4\left(\frac{7\pi}{3}\right)^{1/2} nFy\, D^{1/2}Cr^{2/3}t^{1/6}$$

since,

$$r = \frac{3\alpha}{4\pi} = \frac{3m}{4\pi d}$$

where m is the weight of mercury flowing from the capillary per second, and d is the density of mercury (13.6 g . cm^{-3}).

$$i_t = 0.732\, nFy.D^{1/2}Cm^{2/3}t^{1/6} \qquad \ldots (15)$$

where 0.732 is simply a combination of numerical constants. This is the theoretical equation for the current at any instant t during the life of a mercury drop. This relation was originally derived by Ilkovic.

Equation (15) gives the current in amperes when Fy is expressed in colombs, D in the units $cm^2.Sec^{-1}$., C in terms of moles per cm^3., .m in the units $g.sec^{-1}$ and t in seconds. It is more convenient to express the current in micro amperes, the concentration in terms of millimoles per litre, and m as

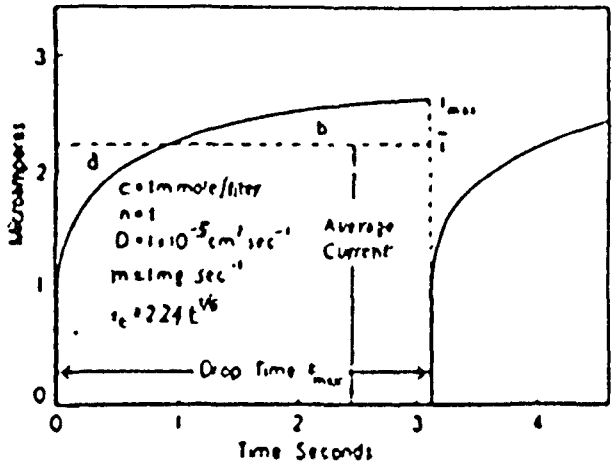

Fig. 14

Theoretical current time curve according to the Ilkovic equation during the formation of an individual mercury drop at the dropping electrode.

$mg.sec^{-1}$ and on this basis when the numerical value of Fy (96,500 colombs) is introduced into eq (15), we have

$$i_t = 706\ nD^{1/2}C\ m^{2/3}t^{1/6} \qquad \text{microamperes} \quad (16).$$

The foregoing equations predict that the current should increase with the sixth root of the time during the life of a drop and hence the current time curve for an individual drop

should be a sixth-order parabola. The theoretical current time curve for a single drop calculated by means of equation (16) for a substance whose diffusion coefficient is $1 \times 10^{-5} cm^2 . sec^{-1}$, a concentration of 1 millimole per litre, a value for m of 1 $mg.sec^{-1}$ and a value for n of 1, is shown in Fig. 14. The area under the current time of a single drop is equal to the quantity of electricity, in microcoulombs, associated with each drop.

In linear diffusion and spherical diffusion to stationary electrodes, the current decreases with time after the e.m.f. is applied, because the concentration gradient at the electrode surface decreases with time. In the case of dropping electrode, the increase of the current with time is due to the fact that the decrease of the concentration gradient at the drop surface is more than compensated by the increase in area of the diffusion field during the life of a drop. The decrease in current due to the decreasing concentration gradient at the drop surface is inversely proportional to the square root, or the three-sixths power, of the time. On the other hand, the increase in current due to the increasing area of the drop is directly proportional to the two-thirds or four-sixths, power of the time. The cumulative results of these two opposite factors is an increase in current according to the one-sixth power of the time.

The average current during the life of a drop is defined as the hypothetical constant current which, following for a length of time equal to the drop time, would produce the same quantity of electricity as the quantity actually associated with each drop. The average current $\bar{I}$, i defined as

$$\bar{I} = \frac{1}{t_{max}} \int_{0}^{t_{max}} i_t \, dt \qquad (17)$$

where t_{max} is the drop time. In view of eq (16)

$$\bar{I} = \frac{706 \; nD^{1/2} cm^{2/3}}{t_{max}} \int_{o}^{t_{max}} t^{1/6} dt \qquad (18)$$

By performing the indicated integration we obtain

$$\bar{I} = 607 \; nD^{1/2} cm^{2/3} t_{max}^{1/6} \qquad (19)$$

This is the equation for the average current which is usually referred to as the 'Ilkovic equation'. It is evident from equation (16) that the maximum current during the life of a drop, at the instant the drop falls, is given by

$$i_{max} = 706 \; nD^{1/2} cm^{2/3} t_{max}^{1/6} \qquad (20)$$

By comparing this equation with (18) or (19) we get

$$\bar{I} = \frac{6}{7} \; i_{max}$$

According to the foregoing relations both the maximum current and the average current are directly proportional to

the concentration of the electroactive substance.

The diffusion currents obtained with the dropping mercury electrode are perfectly reproducible. During the relatively short life of the mercury drops, the concentration gradient around the dropping electrode does not have time to extend very far into the solution, and hence the diffusion layer around the drops is much thinner than that at a stationary spherical micro electrode.

Measurement of Diffusion Currents and Correction for The Residual Current

A small residual current, due to a capacity or charging current plus a small faradaic current resulting from traces of accidental impurities in the solution, is observed before the decomposition potential is reached. In order to obtain the true diffusion current of a substance it is obvious that a correction must be made for this residual current and this correction becomes increasingly more important, the smaller the concentration of the reducible substance, i.e. the smaller the total diffusion current.

When the polarogram of the solution shows only a single wave the most reliable and satisfactory method of evaluating the true diffusion current is an follows [21]. The residual current is determine in a separate experiment by obtaining the

polarogram of the supporting electrolyte solution alone and the value of the residual current so obtained as then subtracted from the total diffusion current of the substance in question. This method is illustrated in Fig. 15, in which the current-voltage curves have been photographically recorded by means of a polarograph.

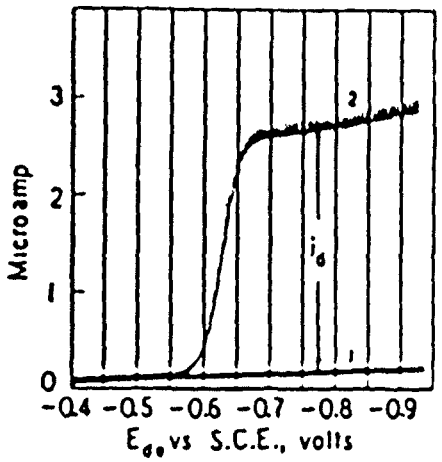

Fig. 15

Extract method of measuring a diffusion current

Curve 1 in the polarogram (residual current) of an air-free O.1N potassium chloride solution which contained 2 x 10^{-5}M sodium methyl red as a maximum suppressor and curve 2 is the polarogram of the same solution containing 5 x 10^{-4}M cadmium chloride. The true diffusion current of the cadmium ion is indicated by 'i_d' and the horizontal line is the 'galvanometer zero line'.

Since the residual current usually increases practically linearly with the applied e.m.f., it is sometimes possible to correct adequately for it by simply extrapolating the residual current section of the curve beyong the decomposition potential, and measuring the distance between this extrapolated line and the total diffusion current.

The extrapolation method is useful when the polarogram in question comprises several waves, as shown in Fig. (16). In this polarogram the diffusion current of the manganous ion can be measured by simply exprapolating the diffusion current of

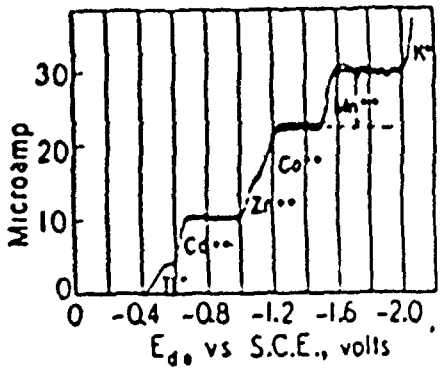

Fig. 16

Polarogram of a solutioncontaining several metal ions

the preceding wave of the cobaltous ion beyond the decomposition of the manganous ion as indicated and measuring the distance between this extrapolated line and the total diffusion current. When the half wave potentials of two substances are close together, so that a well defined diffusion current of the more

easily reducible sustance is not obtained before the reduction of the second substance starts, the measurement of both diffusion currents becomes difficult. This is demonstrated by waves of zinc or cobaltous ions, which are too close together to permit an unambigous evaluation of the two diffusion currents.

CHAPTER - III

EXPERIMENTAL

Although a number of cobalt (II) complexes with amines, amino-acids, and dipeptides are reported to take up oxygen in a reversible manner, the complexes with histidine and diglycine have been investigated in more detail [12, 16, 22, 23]. The cobalthistidine complex absorbs molecular oxygen to form a brown coloured species which is readily decomposed by the addition of acid or by bubbling the solution with nitrogen, releasing thereby obsorbed oxygen. The brown coloured complex is diamagnetic and is probably a binuclear complex.

Complexes of histidine with cobalt (II) in aqueous solution have been examined by proton magnetic resonance spectroscopy [24]. Coordinate interaction of histidine with paramagnetic cobalt (II) produces large contact interaction shifts in the histidine proton resonance spectra. Four histidine cobalt (II) complexes have been distinguished.

Complex I - a weak 1:1 histidine cobalt (II) complex at low pH (<4) in which only the histidine carboxyl group is bonded to octahedral cobalt (II).

Complex II and III - strong 1:1 and 2:1 histidine cobalt (II) complexes at intermediate pH values (4-10) in which hystidine behaves as a tridentate ligand.

Complex IV - a tetrahedral 2:1 histidine cobalt (II)

complex at high pH (>11) in which histidine is bonded to cobalt via the NH_2 group and an imidazole nitrogen atom. It was found that ΔF^{o} for the 2:1 octahedral histidine - cobalt (II) complex composed of one D-histidine and one L-histidine is about 0.7 Kcal/mole less than for the complex containing two histidine ligands of the same configuration (DD or LL). Proton magnetic resonance spectra of complexes of several histidine derivatives with cobalt (II) confirm the structures assigned to the various histidine cobalt (II) complexes.

MATERIALS :

Potassium Nitrate (A.R.) cobalt nitrate (Merck), DL-Methionine (Merck), L-Valine (SRL), DL-Sirine (BDH), L-Alanine (Fluka), Isolucine (Merck), leucine, glycine and L-Asparagine were used without any purification. Double distilled water was used in the preparation of all solutions. Freshly prepared solutions of amino-acids were used.

POLAROGRAPHIC STUDIES :

The polarographic studies of reaction between cobalt (II) and amino-acid were carried out at room temperature by polarographic Analyser (EG and Parc. Model 264A). The solutions of KNO_3, cobalt (II) and amino acid were introduced in the polarographic cell. Oxygen was removed by bubbling nitrogen gas through the solution. The purification of nitrogen gas was

done by passing the gas through three vessels containing the solution of chromous chloride, alkaline pyragallol solution and the concentrated sulphuric acid for absorbing the moisture from the nitrogen gas.

Figures 1-7 represent the plots of applied potential versus current for the reaction of cobalt (II) with various amino-acids.

Each set of plots was obtained by keeping constant, the concentration of cobalt (II) at 0.00025M and potassium nitrate at 0.03252M and that of amino-acid was varied. Total volume of the solution in the cell was kept constant by adding double distilled water. Nitrogen gas was bubbled for 8 minutes in the cell containing the solutions. The curves were recorded in the potential range 1.00 volt to 2.00 volt, scan rate 5 mv/sec and current range was 10μA.

Fig. 1 represents the plots of applied potential versus current for the reaction of cobalt (II) with α-Alanin. Curve A was obtained by taking 0.00025M of cobalt (II), 0.0325M of KNO_3 and keeping the concentration of α-Alanine zero. The potential curve was taken and its $E_{1/2}$, calculated. Then curve B was obtained by taking 0.625M of α-Alanine and keeping the concentration of cobalt (II) and KNO_3 same as in the case of curve A.

The same excercise was repeated for curves C, D, E and F by taking 0.125M, 0.25M, 0.375M and 0.05M of α-Alanine respectively.

Figure 2 was obtained similarly with isoleucine curves A, B, C, D and E were obtained by keeping the concentration of the amino-acid 0, 0.0208M, 0.041M, 0.0833M and 0.125M respectively.

The same exercise was repeated with Methionine to obtain Fig. 3.

In Figure 4, curves A, B, C, D and E were obtained by using 0, 0.08M, 0.16M and 0.25M of serine.

In figure 5, the amino-acid selected was L-valine. 0 , 0.0208M, 0.041M, 0.0833M and 0.125M of valine were used to obtain curves A, B, C, D and E.

Similarly figure 6 was obtained with Asparagine and Figure 7 with glycine. The values of $E_{1/2}$ calculated on the basis of the curves in fig. 1, 2, 3, 4, 5, 6 and 7 are reported in the Tables I, II, III, IV, V, VI and VIII.

KINETIC STUDIES :

The rate constant was calculated with the stopped flow spectrometer (Hi. tech support unit SF-3L). A cobalt histidine

complex solution was prepared in which the concentration of cobalt (II) was 0.1M and that of histidine was 0.25M. This complex solution was taken in one syringe and 0.25M of ETDA in another syringe. The syringe plungers were then driven rapidly. The two solutions from the two syringes come out in the form of very fast streams and are mixed in the mixing chamber. From the mixing chamber the solution passes at once into the reaction cuvette. The curves were directly recorded by the computer, which is reproduced in the Fig. 8.

Subsequent extensions to other ligands have been rather not well established owing to unidentification of the red complexes of monomeric cobalt (III) obtained from the over all oxidation reactions, as oxygenated intermediate, especially in the case of amino acids other than histidine. Oxygenation of the bis (histidine) complex of cobalt (II) to give brown binuclear oxygenated complexes is too fast to employ stopped flow technique to measure the rates [25]. This problem is undertaken precisely to understand for a variety of amino acids, the requirement and conditions for oxygenation and oxidation of cobalt (III) amino acid complexes.

CHAPTER - IV

RESULTS AND DISCUSSION

Table no. 1 describes the results for cobalt (II) with α-Alanine in presence of nitrogen i.e. in absence of oxygen. The half-wave potential for cobalt (II) ion in absence of α-Alanine comes at 1.08 volts. The cobalt ion half wave potential in presence of varying concentration of α-Alanine, keeping Co^{++} ion concentration constant, comes at 0.98 volt. It appears that the change of α-Alanine concentration does not affect the value of half wave potential, which in all cases are 0.98 volt. We conclude therefore that the composition of the complex formed in the absence of oxygen is same irrespective of the concentration of the ligand, α-Alanine.

Table no. 2 represents the results for cobalt (II) with isoleucine in absence of oxygen. The result is given exactly in the pattern of Co^{++} with α-Alanine described as above. The Co^{++} ion half wave potential in absence of isoleucine is at 1.08 volt, while addition of isoleucine in varying concentration, decreases this value to 1.00 volt which remains constant. It shows that again the cobalt - isoleucine complex is formed having a single composition. However, the complex forming tendency of isoleucine is comparatively weaker than that of α-Alanine with cobalt, as indicated by the values of half-wave potential.

Similarly the formation of complex with cobalt by several other amino acids, namely Methionine, Valine, Serine, Asparagine

and Glycine have been studied and the results are reported in tables 3, 4, 5, 6 and 7 along with the half-wave potentials. From the values of the half-wave potentials, it is quite apparent that the complex formation with Co^{++} ion is taking place in good measure with Methionine, Valine, and to a negligible extent with Serine, Asparagine and Glycine under the given conditions.

We have started the study by confirming the previous observation [12], that the complex formed between cobalt (II) and L-histidine absorbs oxygen, and involve the equilibrium

$$2\ Co(L\text{-}h)_2 + O_2 \rightleftharpoons [Co(L\text{-}h)_2]_2O_2$$

The bis (L-histidinato) cobalt (II) $-O_2$ complex has the absorption peaks at 385 mμ and 350 mμ; which are in agreement with the reported value. The freshly formed brown species was decomposed by EDTA. The loss of brown colour on addition of EDTA to an oxygenated cobalt (II) - histidine solution show the first order kinetics. Separate experiments show that EDTA reacts redily with Coh_2 to form a species which is not oxygen sensitive. It only indicates that EDTA acts by removing Coh_2 and possibly $Co(h_2)\ O_2$ present in the equilibria given above.

The study of the other Co-amino acids complex could not be carried out at the moment because the stopped flow spectrometer has gone out of order, and is currently under repair.

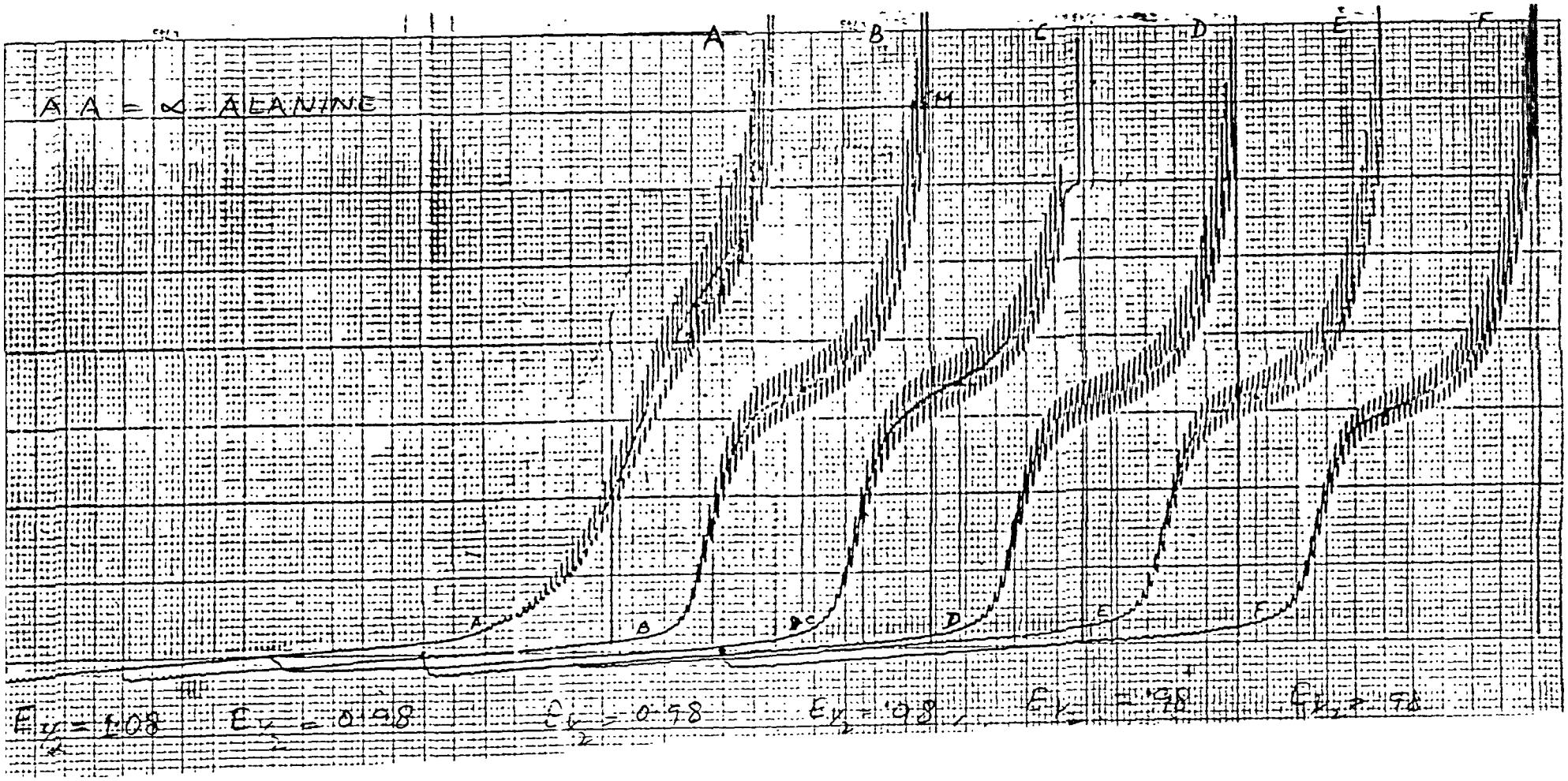

Fig. 1.

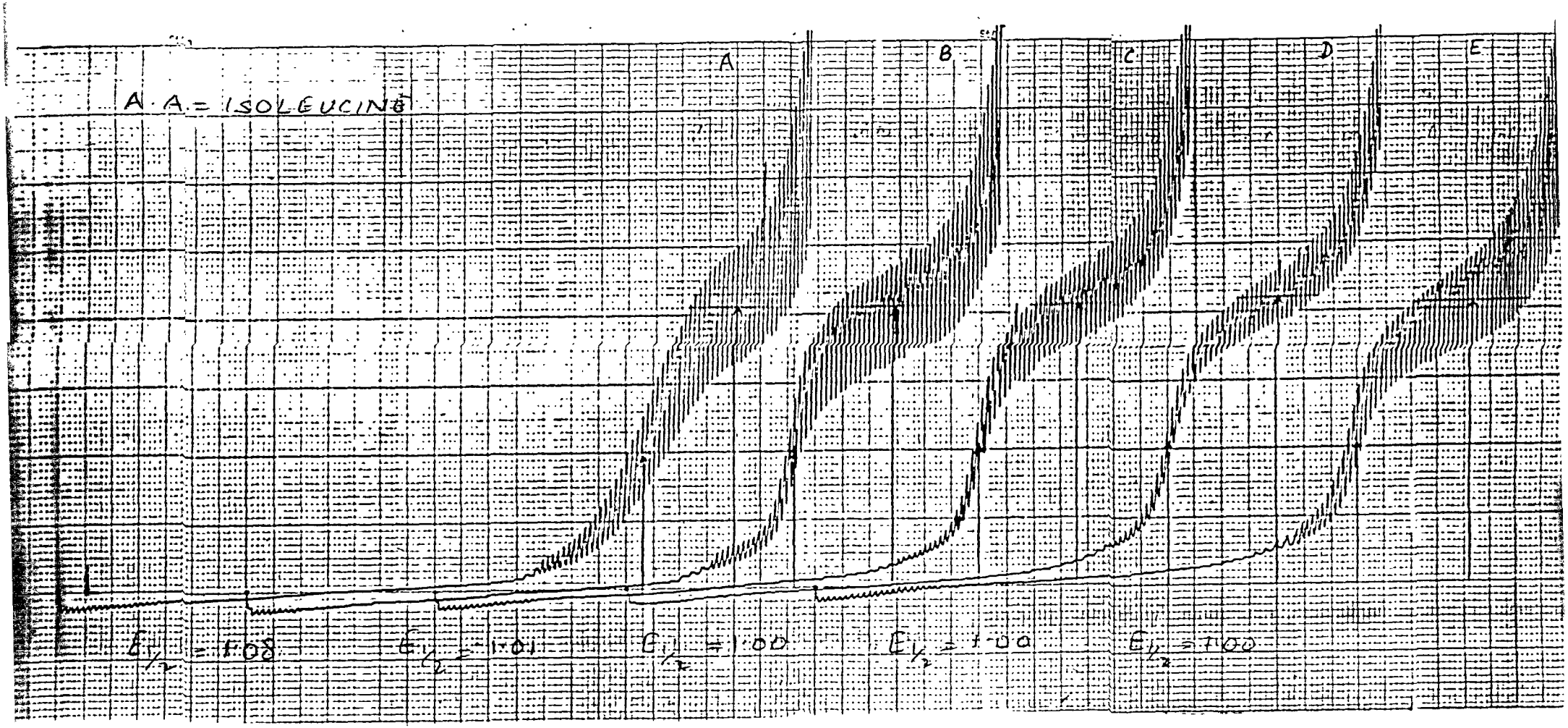

Fig 2.

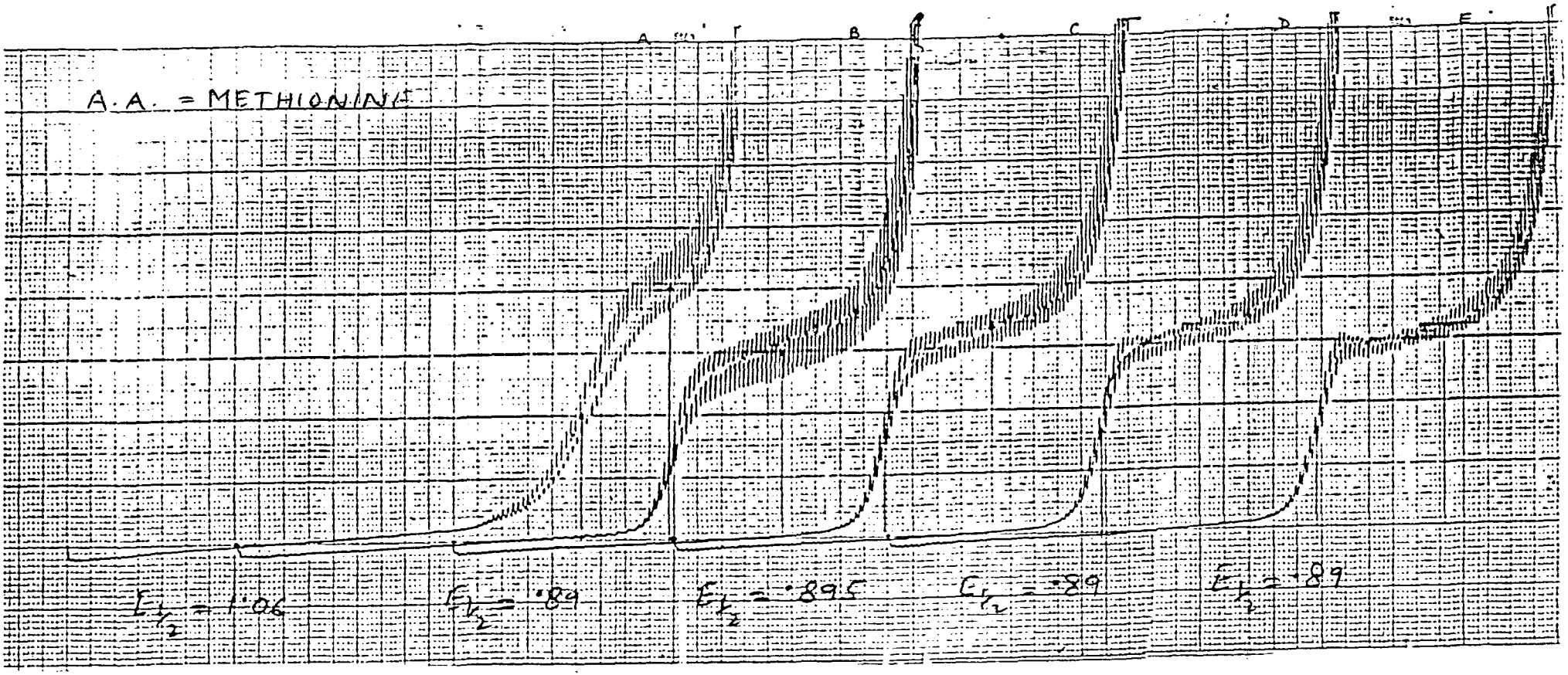
A.A. = METHIONINE
A
B
C
D
E
$E_{\frac{1}{2}} = 1.06$
$E_{\frac{1}{2}} = .89$
$E_{\frac{1}{2}} = .895$
$E_{\frac{1}{2}} = .89$
$E_{\frac{1}{2}} = .89$

Fig 3

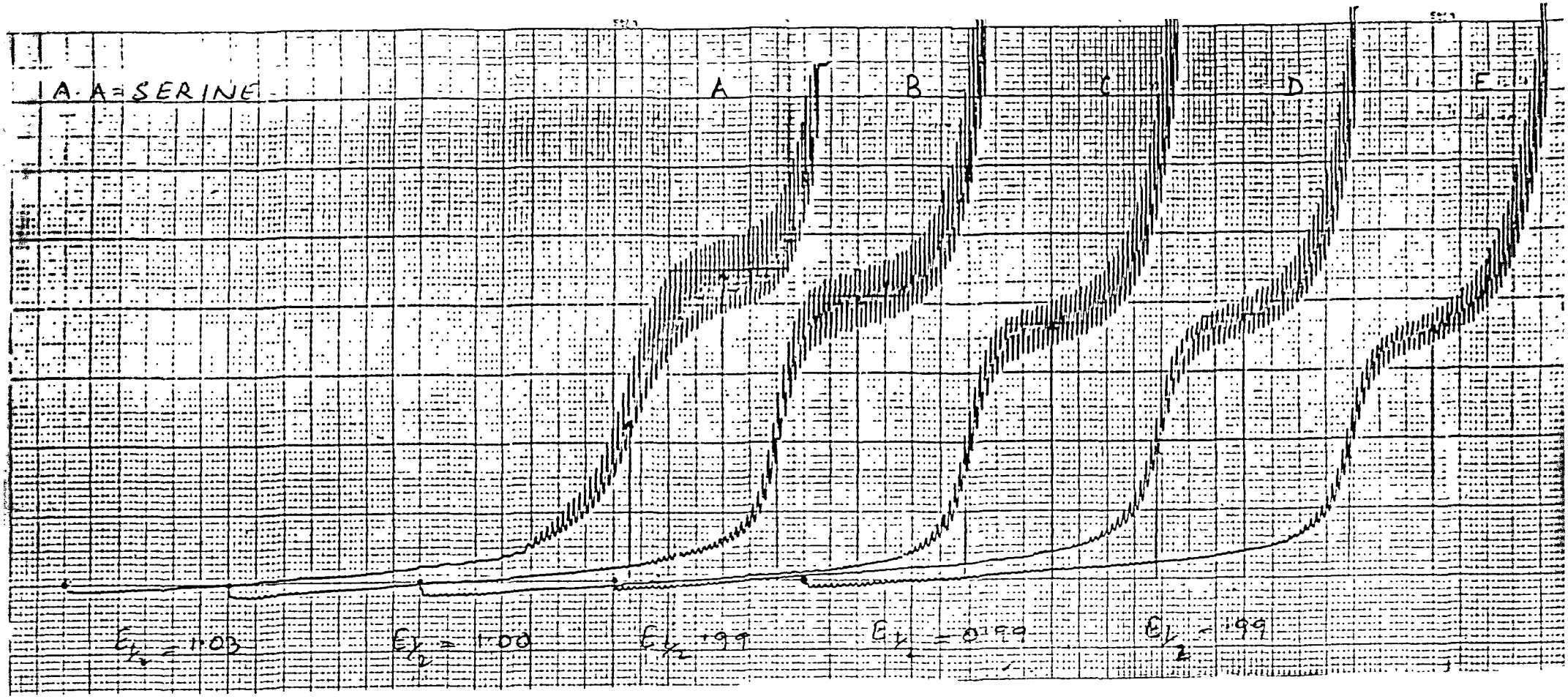
A. A=SERINE
A
B
C
D
E
$E_{\frac{1}{2}} = 1.03$
$E_{\frac{1}{2}} = 1.00$
$E_{\frac{1}{2}} = .99$
$E_{\frac{1}{2}} = 0.99$
$E_{\frac{1}{2}} = .99$

Fig 4.

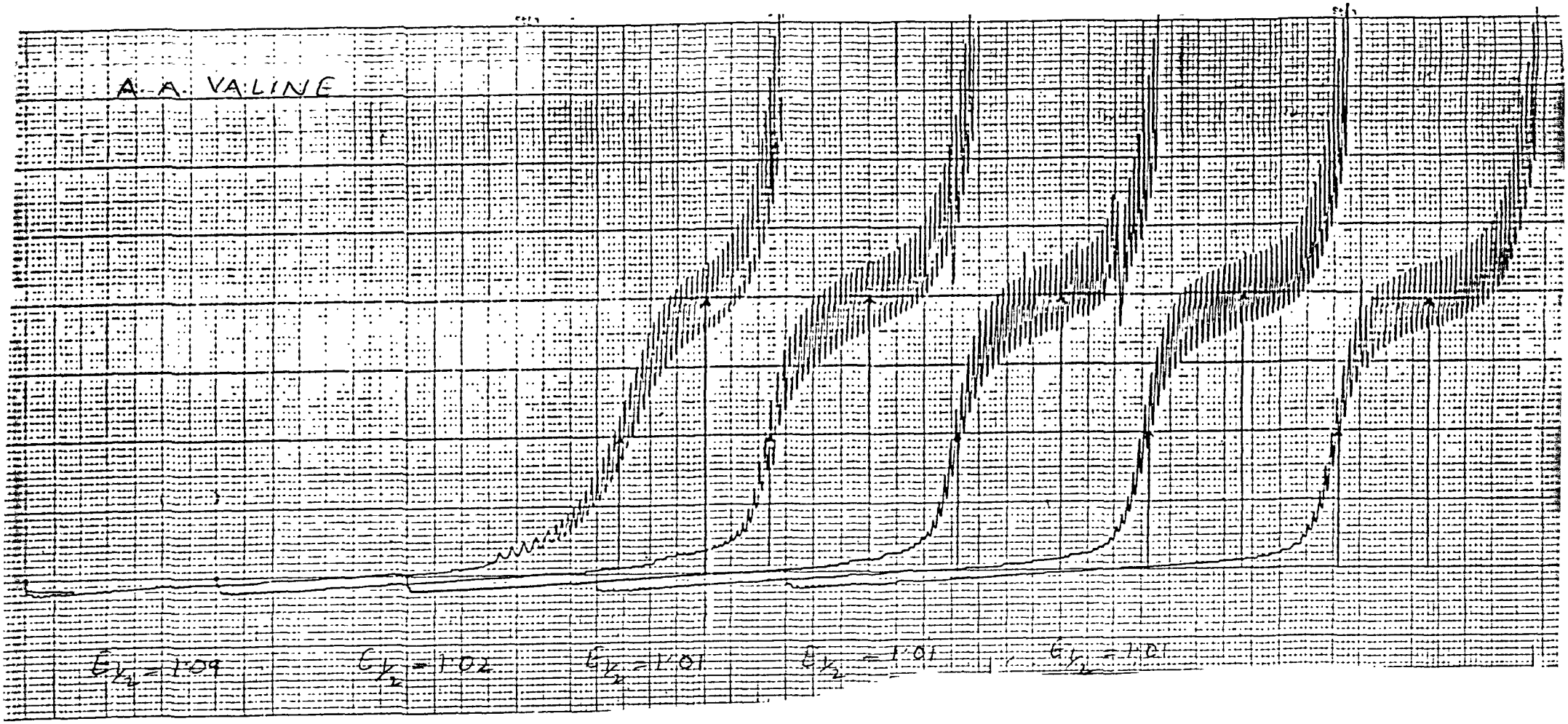

Fig 5.

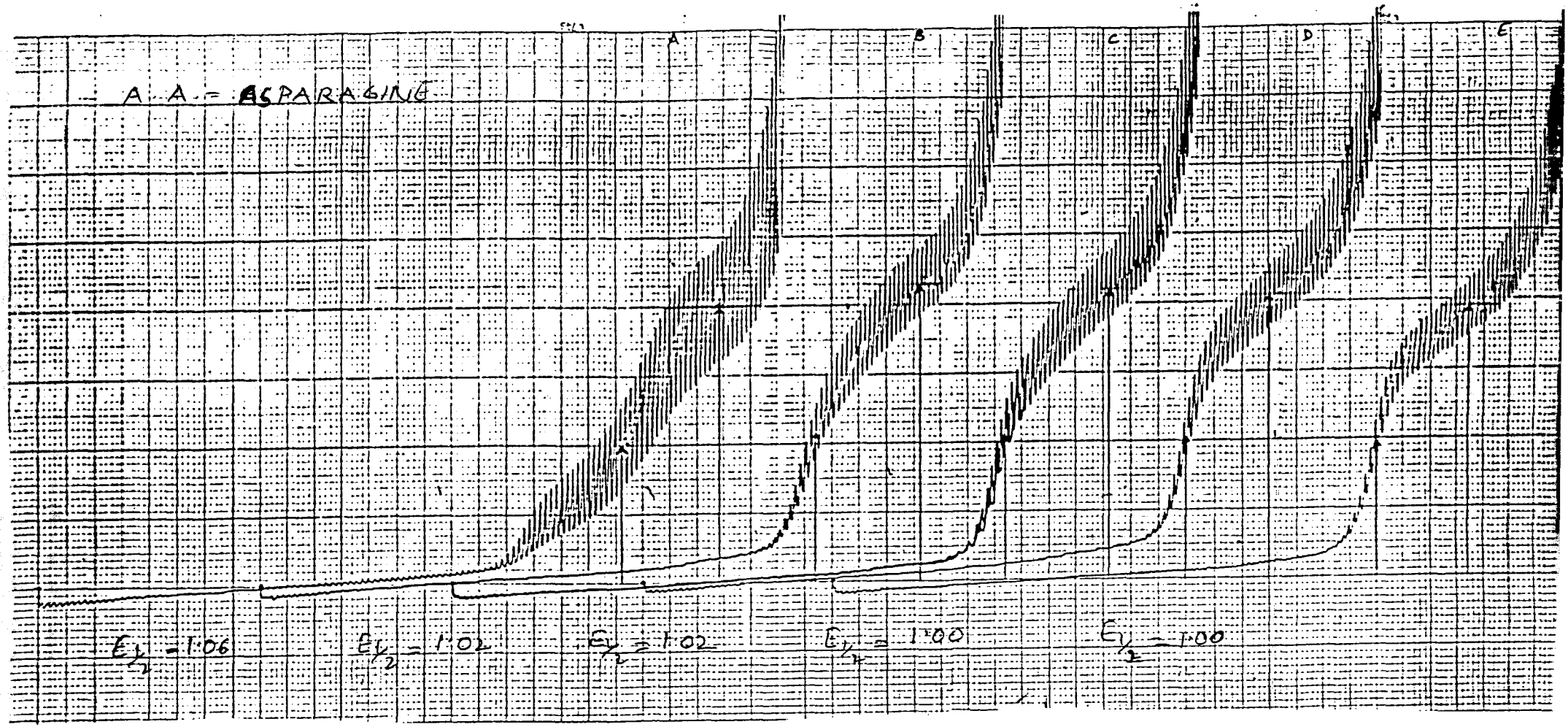

Fig. 6.

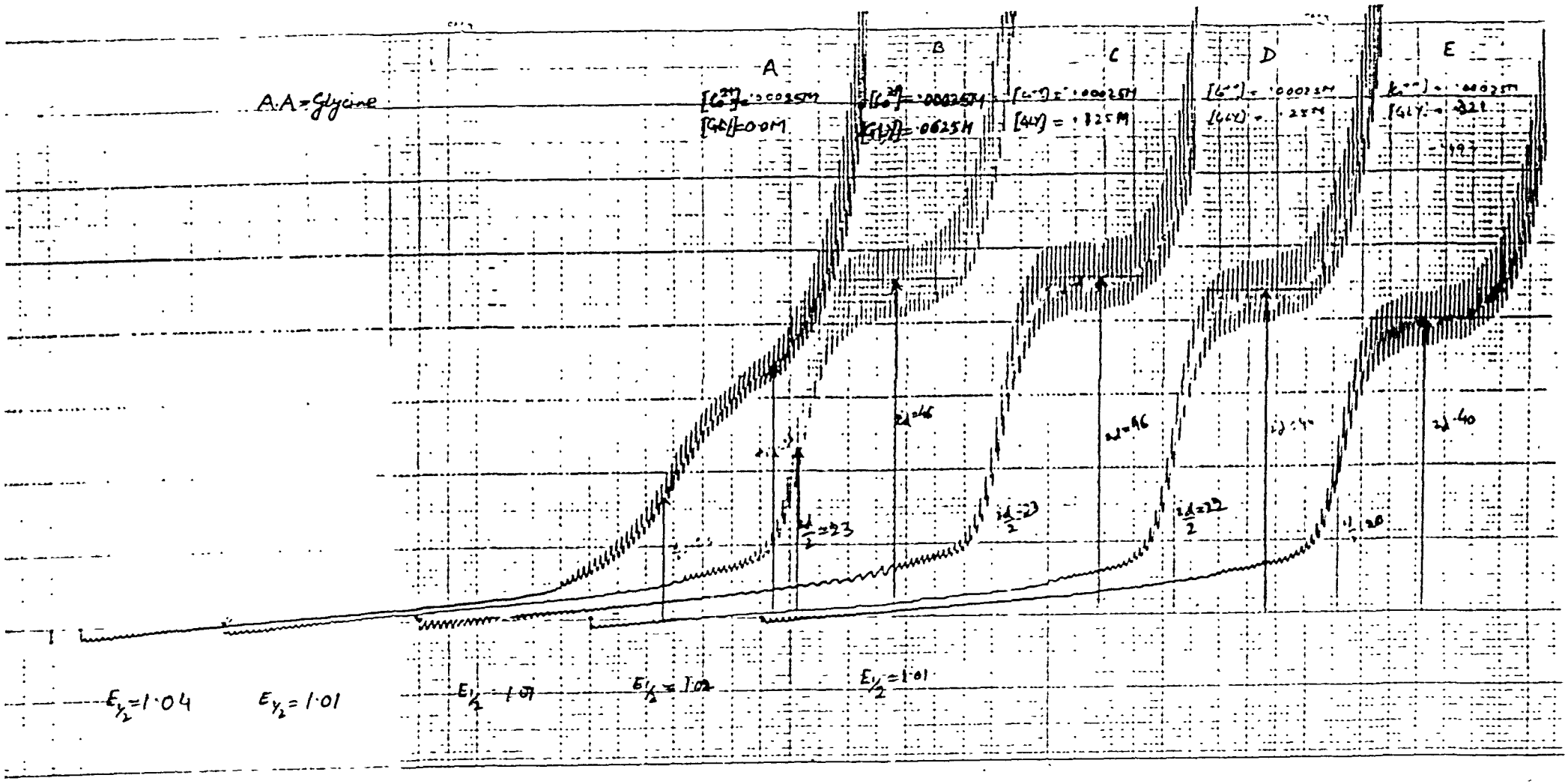

Fig 7

TABLE No. 1

VARIATION OF α-ALANINE IN ABSENCE OF O_2, CURRENT RANGE = 10 μA SCAN RATE = 5mv/sec

S.No.	COMPOSITION	CONCENTRATION of Co^{++}	CONCENTRATION of α-ALANINE	HALF-WAVE POTENTIAL	DIFFUSION CURRENT
1	15 ml KNO_3 + 15 ml H_2O + 0.5 ml Co^{++} + 0 ml ALANINE	0.00025M	0M	1.08	45
2	15 ml KNO_3 + 13.1 ml H_2O + 0.5 ml Co^{++} + 1.9 ml ALANINE	0.00025M	0.0625M	0.98	34
3	15 ml KNO_3 + 11.25 ml H_2O + 0.5 ml Co^{++} + 3.75 ml ALANINE	0.00025M	0.125M	0.98	34
4	15 ml KNO_3 + 7.5 ml H_2O + 0.5 ml Co^{++} + 7.5 ml ALANINE	0.00025M	0.25M	0.98	34
5	15 ml KNO_3 + 3.75 ml H_2O + 0.5 ml Co^{++} + 11.25 ml ALANINE	0.00025M	0.375M	0.98	32
6	15 ml KNO_3 + 0 ml H_2O + 0.5 ml Co^{++} + 15 ml ALANINE	0.00025M	0.5M	0.98	31

TABLE No. 2

VARIATION OF ISOLEUCINE IN ABSENCE OF O_2, CURRENT RANGE = 10μA SCAN RATE = 5mv/sec

S.No.	COMPOSITION	CONC. of Co^{++}	CONC. of ISOLEUCIN	HALF-WAVE POTENTIAL	DIFFUSIO CURRENT
1	15 ml KNO_3 + 15 ml H_2O + 0.5 ml Co^{++} + 0 ml ISOLEUCINE	0.00025M	OOM	1.08	41
2	15 ml KNO_3 + 13.75 ml H_2O + 0.5 ml Co^{++} + 1.25 ml ASOLEUCINE	0.00025M	0.0208M	1.01	41
3	15 ml KNO_3 + 12.5 ml H_2O + 0.5 ml Co^{++} + 2.5 ml ISOLEUCINE	0.00025M	0.041M	1.00	41
4	15 ml KNO_3 + 10 ml H_2O + 0.5 ml Co^{++} + 5 ml ISOLEUCINE	0.00025M	0.0833M	1.00	42
5	15 ml KNO_3 + 7.5 ml H_2O + 0.5 ml Co^{++} + 7.5 ml ISOLEUCINE	0.00025M	0.0125M	1.00	41

TABLE No. 3

VARIATION OF METHIONINE IN ABSENCE OF O_2, CURRENT RANGE = 10μA SCAN RATE = 5mv/sec

S.No.	COMPOSITION	CONC. of Co^{++}	CONC. of METHIONINE	HALF-WAVE POTENTIAL	DIFFUSION CURRENT
1	15 ml KNO_3 + 15 ml H_2O + 0.5 ml Co^{++} + 0 ml METHIONINE	0.00025M	00M	1.06	41
2	15 ml KNO_3 + 13.75 ml H_2O + 0.5 ml Co^{++} + 1.25 ml METHIONINE	0.00025M	0.0208M	0.89	30
3	15 ml KNO_3 + 12.5 ml H_2O + 0.5 ml Co^{++} + 2.5 ml METHIONINE	0.00025M	0.041M	0.895	34
4	15 ml KNO_3 + 10 ml H_2O + 0.5 ml Co^{++} + 5.0 ml METHIONINE	0.00025M	0.0833M	0.89	33
5	15 ml KNO_3 + 7.5 ml H_2O + 0.5 ml Co^{++} + 7.5 ml METHIONINE	0.00025M	0.125M	0.89	32

TABLE No. 4

VARIATION OF SERINE IN ABSENCE OF O_2, CURRENT RANGE = 10μA SCAN RATE = 5mv/sec

S.No.	COMPOSITION	CONC. of Co^{++}	CONC. of SERINE	HALF-WAVE POTENTIAL	DIFFUSION CURRENT
1	15 ml KNO_3 + 15 ml H_2O + 0.5 ml Co^{++} + Oml SERINE	0.00025M	OOM	1.03	45
2	15 ml KNO_3 + 12.5 ml H_2O + 0.5 ml Co^{++} + 25 ml SERINE	0.00025M	0.041M	1.00	41
3	15 ml KNO_3 + 10.2 ml H_2O + 0.5 ml Co^{++} + 4.8 ml SERINE	0.00025M	0.08M	0.99	37
4	15 ml KNO_3 + 5.4 ml H_2O + 0.5 ml Co^{++} + 9.6 ml SERINE	0.00025M	0.16M	0.99	38
5	15 ml KNO_3 + O ml H_2O + 0.5 ml Co^{++} + 15 ml SERINE	0.00025M	0.25M	0.99	36

TABLE No. 5

VARIATION OF VALINE IN ABSENCE OF O_2, CURRENT RANGE = 10μA SCAN RATE = 5mv/sec

S.No.	COMPOSITION	CONC. of Co^{++}	CONC. of VALINE	HALF-WAVE POTENTIAL	DIFFUSION CURRENT
1	15 ml KNO_3 + 15 ml H_2O + 0.5 ml Co^{++} + Oml VALINE	0.00025M	OOM	1.09	40
2	15 ml KNO_3 + 13.75 ml H_2O + 0.5 ml Co^{++} + 1.25 ml VALINE	0.00025M	0.0208M	1.02	40
3	15 ml KNO_3 + 12.5 ml H_2O + 0.5 ml Co^{++} + 2.5 ml VALINE	0.00025M	0.041M	1.01	40
4	15 ml KNO_3 + 10.0 ml H_2O + 0.5 ml Co^{++} + 5.0 ml VALINE	0.00025M	0.0833M	1.01	40
5	15 ml KNO_3 + 7.5 ml H_2O + 0.5 ml Co^{++} + 7.5ml VALINE	0.00025M	0.125M	1.01	40

TABLE No. 6

VARIATION OF ASPARAGINE IN ABSENCE OF O_2, CURRENT RANGE = 10μA SCAN RATE = 5mv/sec

S.No.	COMPOSITION	CONC. of Co^{++}	CONC. of ASPARAGINE	HALF-WAVE POTENTIAL	DIFFUSION CURRENT
1	15 ml KNO_3 + 15 ml H_2O + 0.5 ml Co^{++} + 00ml ASPARAGINE	0.00025M	00M	1.06	40
2	15 ml KNO_3 + 13.9 ml H_2O + 0.5 ml Co^{++} + 1.1 ml ASPARAGINE	0.00025M	0.0185M	1.02	43
3	15 ml KNO_3 + 12.78 ml H_2O + 0.5 ml Co^{++} + 2.22 ml ASPARAGINE	0.00025M	0.037M	1.02	42
4	15 ml KNO_3 + 10.56 ml H_2O + 0.5 ml Co^{++} + 4.44 ml ASPARAGINE	0.00025M	0.074M	1.00	41
5	15 ml KNO_3 + 8.34 ml H_2O + 0.5 ml Co^{++} + 6.66 ml ASPARAGINE	0.00025M	0.111M	1.00	39

TABLE No. 7

VARIATION OF GLYCINE IN ABSENCE OF O_2, CURRENT RANGE = 10 μA SCAN RATE = 5 mv/sec

S.No.	COMPOSITION	CONC. of Co^{++}	CONC. of GLYCINE	HALF-WAVE POTENTIAL	DIFFUSION CURRENT
1	15 ml KNO_3 + 15 ml H_2O + 0.5 ml Co^{++} + Oml GLYCINE	0.00025M	OOM	1.04	35
2	15 ml KNO_3 + 13.1 ml H_2O + 0.5 ml Co^{++} + 1.89 ml GLYCINE	0.00025M	0.0625M	1.01	46
3	15 ml KNO_3 + 11.25 ml H_2O + 0.5 ml Co^{++} + 3.75 ml GLYCINE	0.00025M	0.125M	1.01	46
4	15 ml KNO_3 + 7.5 ml H_2O + 0.5 ml Co^{++} + 7.5 ml GLYCINE	0.00025M	0.25M	1.02	44
5	15 ml KNO_3 + 5.4 ml H_2O + 0.5 ml Co^{++} + 9.6 ml GLYCINE	0.00025M	0.321M	1.01	40

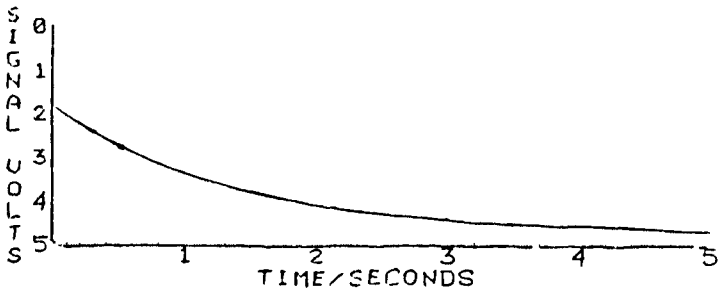

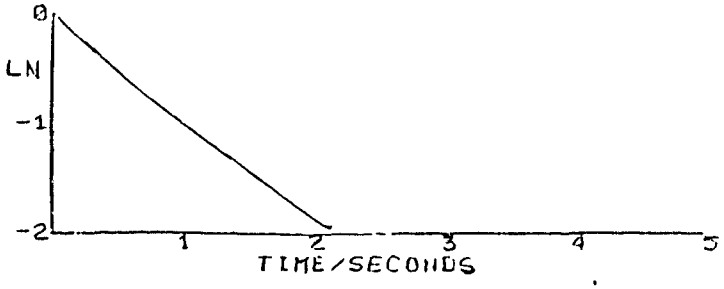

RATE CONSTANT=.9229 (1/SEC)
STANDARD DEVIATION = (+/-).01

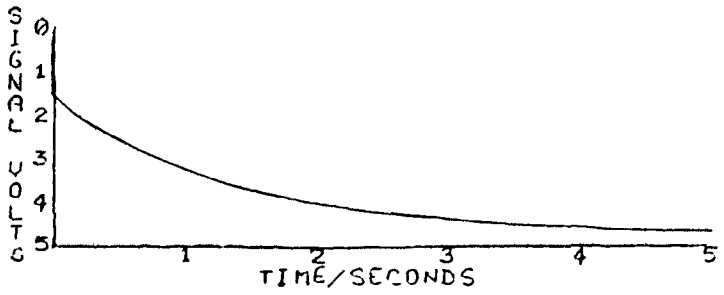

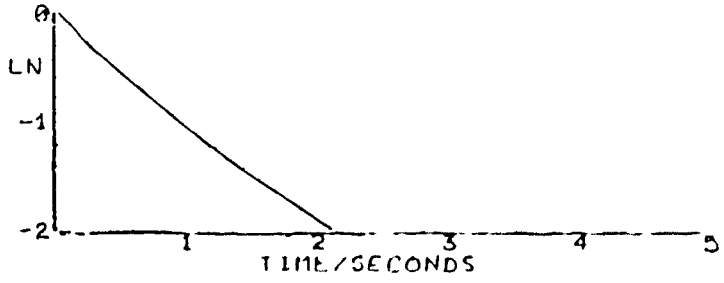

RATE CONSTANT=.9225 (1/SEC)
STANDARD DEVIATION = (+/-).01

REFERENCES

1. Pfeiffer, Breith, Lubbe and Tsumaki, Ann., 503, 84 (1933).

2. Tsumaki, Bull. Chem. Soc., Japan, 13, 252 (1938).

3. Calvin, Bailes and Wilmarth, J. Am. Chem. Soc., 68, 2254 (1946).

4. Barkelew and Calvin, J. Am. Chem. Soc., 68, 2254 (1946).

5. Wilmarth, Aranaff and Calvin, J. Am. Chem. Soc., 68, 2263 (1946).

6. Hughes, Wilmarth and Calvin, J. Am. Chem. Soc., 68, 2273 (1946).

7. Harle and Calvin, J. Am. Chem. Soc., 68, 2612 (1946).

8. Burke, Hearon, Caroline and Schade, J. Biol. Chem., 165, 723 (1946).

9. A.E. Martell and Calvin, Chemistry of the metal chelate compounds, p. 336. Prentice - Hall, New York (1952).

10. D. Burk, A.L. Schade, M.L. Hesselbach and C.R. Fischer, Federation Proc., 5, 1266 (1946).

11. E.L. Smith, J. Biol. Chem., 173, 571 (1948).

12. J.Z. Hearon, D. Burk and Schade, J. Nat. Cancer Inst. 9, 337 (1949).

13. J.B. Gilbert, M. Clydeotey and V.E. Price, J. Biol. Chem., 190, 377 (1950).

14. V.E. Price, A. Meister, J.B. Gilbert and J.P. Greenstein, J. Biol. Chem., 181, 535 (1949).

15. Burk, D. Fiala, Federation Proc., 7, 148 (1948).

16. Charles Janford, D.C. Kirk Jr. and M.K. Chantooni, J. Am. Chem. Soc., 76, 5325 (1954).

17. K.J. Laidler, Chemical Analysis, p. 33, Harper and Row, Publishers, New York (1987).

18. G.W. Castellan, Physical Chemistry, p. 828, Narosa Publishing House, Delhi (1988).

19. A.M. Bond, Marsal and Decors, Modern Polarographic Methods in Analytical Chemistry (1980).

20. J.J. Lingane and I.M. Kolthoff, Polarography (1965).

21. J.J. Lingane and I.M. Kolthoff, J. Am. Chem. Soc., 61, 825 (1939).

22. Y. Caglioti, P. Silvestroni and C. Furlani, J. Inorg. Nucl. Chem., 13, 95 (1960).

23. Y. Sano and H. Tanabe, ibid, 25, 11 (1963).

24. C.C. McDonald and W.D. Philips, J. Am. Chem. Soc., 85, 3736 (1963).

25. J. Simplicio and R.G. Willkins, ibid, 89, 6092 (1967).